# Chapter 1

# Introduction

## 1.1 BACKGROUND

The behaviour of soils in general can be modelled using two types of approach, namely the phenomenological approach and the structural approach (Feda, 1982). The former is considered on the basis of continuum theories, such as elasticity and plasticity, in which a material is replaced by a mathematical model of a structure-less continuum. Numerous models have been derived from studies involving remoulded and reconstituted soils. According to a model such as critical state soil mechanics, soil behaviour is described by the initial void ratio and its subsequent modification due to stress history (Vaughan, 1985; Vaughan et al., 1988). It is assumed that the soil deforms homogeneously during shear, reaching a critical state at large strains, regardless of the initial testing conditions.

An alternative approach is the structural approach. The behaviour of the soil is modelled on the basis of interactions between discreet particles, and any structural features would influence the behaviour of the soil. If every single particle is modelled with its own load conditions, the exact results can be obtained. This is however not possible with current technology and the solution must be estimated from a balance of the two approaches.

There have been differences in the definition of the terms ‘structure’ and ‘fabric’. According to Terzaghi and Peck (1948), the term ‘structure’ is defined as ‘the pattern in which soil particles are arranged in the aggregate’ and according to Mitchell (1956), ‘fabric’ is defined as ‘the appearance of

patterns produced by shapes and arrangement of the mineral grains'. Rowe (1972) defined 'fabric' as the size, shape and arrangement of solid particles, the organic inclusions and the associated voids while 'structure' is associated with arrangement of a particular size range. According to Lambe and Whitman (1969) and Mitchell (1976), 'structure' is defined as a combination of particle arrangement (fabric) and bonding (inter-particular forces, including cementation, electrostatic, electromagnetic or any other force which keeps the particles together). In the context of this thesis, this latter definition is adopted. 'Fabric' defines the arrangement of particles and associated pores while 'structure' defines the combination of fabric and bonding.

In the past two decades, researchers such as Mulilis et al. (1977), Keurbis et al. (1988), Vaid et al. (1990), Ishihara (1993), Zlatovic and Ishihara (1997), Chillarige et al. (1997), Dyvik and Hoeg (1999) and Vaid et al. (1999) have shown that the behaviour of a non-plastic, cohesionless soil produced using different reconstituted methods, but tested at the same state and loading conditions may be significantly different. They speculate that this difference in behaviour is a result of the different fabric which ensues upon sample preparation. This is in direct conflict with models such as the critical state model, which suggests that the behaviour of a soil is only dependent upon its current void ratio, mean effective stress and deviatoric stress. Natural soils differ from reconstituted soils on both micro and macro scales owing to the fabric. It is therefore important that fabric effects be understood and incorporated in the interpretation of laboratory test results.

Although tailings dams have been constructed for over a century in South Africa, relatively little is known about their behaviour. Predictions are often based on empirical observations or simple calculations from limited information. Tailings dams pose a potential threat to the environment in the event of a failure e.g. the failures at Bafokeng in 1974 and Merriespruit in 1994. Although failures of this magnitude are rare, they nevertheless impose significant potential risk to both the public and mining companies. Unless the understanding of tailings behaviour is advanced, these threats will remain in existence. Due to the complexity of undisturbed sampling of tailings,

predictions of the behaviour of tailings are generally based on controlled laboratory tests on reconstituted samples. Although many sample reconstitution methods are available, it is not clear which reconstitution method, if any, will present behaviour representative of in situ conditions.

## 1.2 OBJECTIVE

The objective of this research is to examine the behaviour of undisturbed and reconstituted gold tailings samples at the same state (void ratio and effective stress). It is postulated that samples constructed by different laboratory preparation methods will produce different particle arrangement (fabric) and will behave differently at the same state. Undisturbed samples will be compared to laboratory reconstituted samples to evaluate the similarities and differences in behaviour and fabric.

## 1.3 SCOPE

The extent of this study was limited due to the complex nature of tailings and soils in general. The limitations can be summarized as follows:

- The material was limited to gold tailings from ERPM dam 4.
- All samples were surface samples obtained within a depth of 1 metre.
- The research was laboratory based.
- Investigation of behaviour included sedimentation, collapse and swell, isotropic consolidation, creep, undrained shear and stiffness.
- Only saturated conditions were considered. Although in situ samples near the surface may have been de-saturated during desiccation, all triaxial tests were conducted on saturated in situ or laboratory reconstituted samples.
- The study concentrated on the physical properties of gold tailings particles and their influence on the mechanical behaviour of gold tailings. Mechanical behaviour is defined by Olson and Mesri (1970) as mechanical

bending, compressing and rupture of the particles coupled with shearing displacement at particle contacts. Although it is recognized that pore fluid chemistry plays an important role, all triaxial tests were conducted using de-aired tap water. Distilled water was used for sample preparation of slurry and moist tamped samples. In some cases, dispersant or flocculants were used to obtain the required void ratio. For these cases, an additional flushing process was incorporated to eliminate as much of the dispersant as possible. An assumption was made that the dispersant or flocculants had an effect only on the resulting fabric, and not on the mechanical behaviour of the tailings.

- The main aim of the research was to investigate the effect of particle arrangement (fabric) on the mechanical behaviour of gold tailings. Effects of factors such as fines content and particle shape which are known to influence the behaviour, were not controlled, but assumed to be constant for a particular sampling position.

## 1.4 METHODOLOGY

A hypothesis was proposed as a guideline for this study. The hypothesis states that: **Accurate simulation of the behaviour of gold tailings under laboratory conditions requires appropriate replication of the material fabric.** In order to validate the hypothesis, the tailings samples were subjected to a number of controlled laboratory tests. Testing can be summarized as follows:

- Indicator tests included particle size distribution, specific gravity and Atterberg limits.
- Maximum and minimum void ratio tests to establish void ratio limits for the tailings.
- Sedimentation tests with dispersant and flocculants
- Triaxial consolidation.

- Undrained triaxial tests on in situ and laboratory samples. Instrumentation included external displacement transducer, internal submersible load cell and LVDTs to measure local axial strain.
- Image analysis of in situ and laboratory prepared samples. This included the use of scanning electron microscopy (SEM) on naturally desiccated samples.

A method of fabric differentiation, based on SEM images, will be established. The method could be qualitative or quantitative. This allows some conclusions to be drawn about fabric and behaviour of gold tailings.

## 1.5 ORGANIZATION OF THESIS

The thesis consists of the following chapters:

- Chapter 1 serves as the introduction to the thesis.
- Chapter 2 presents the existing knowledge on gold tailings and reviews current methods and relevant information on fabric analysis.
- Chapter 3 discusses all experimental work including testing strategy, processes and procedures.
- Chapter 4 presents the fabric of gold tailings and methods of classification relevant to the behaviour of gold tailings.
- Chapter 5 discusses the analysed data in terms of the effect of particle arrangement (fabric) on the mechanical behaviour of in situ and laboratory prepared gold tailings.
- Chapter 6 closes the thesis with a summary of the main conclusions, recommendations for laboratory testing in industry and suggestions for further research based on the results of this thesis.
- Chapter 7 lists all references used in the thesis.
- Appendix A includes the preliminary SEM imagess.
- Appendix B consists of all instrumentation data as well as calibration graphs.

- Appendix C describes all sample preparation procedures.
- Appendix D includes all SEM images used for fabric classification.
- Appendix E presents all results obtained for the experimental programme. This includes the preliminary tests and the consolidation and shear tests.

# Chapter 2

# Literature Review

## 2.1 INTRODUCTION

The objective of the literature review is to present the available literature on the research topic. This provides the basis from which the experimental programme was developed. The first sections are dedicated to the description of gold tailings in general. The geology and mineralogy of the Witwatersrand gold reef, which is the primary source of the tailings used in this research, is discussed. This is followed by a brief discussion of the processes involved in gold extraction and general design and construction of tailings dams in South Africa. The engineering properties of gold tailings from documented literature are also presented. Discussion of soil fabric is introduced with documented differences in behaviour, followed by detailed literature on available methods of fabric measurement and analysis. As laboratory sample preparation is a significant part of this research, a detailed discussion on available methods of laboratory sample preparation is included. This is followed by a brief discussion on sampling and sample disturbance. The chapter is concluded with a summary of the literature review.

## 2.2 GEOLOGY AND MINERALOGY OF THE WITWATERSRAND GOLD REEF

The Witwatersrand goldfields were laid down between 2.7 and 3 billion years ago, in an oval area approximately 42 000km², in the Gauteng, North-West and Free State provinces of South Africa. Sediments originating from the

surrounding Archian granite-greenstone terrains were deposited in a large basin and through compression and chemical processes formed the gold-bearing rock body (Stanley, 1987). Detrital particles in the deposit underwent low-grade metamorphism which led to re-crystallization, thus forming gold. Gold ores in the Witwatersrand goldfields exist in sheets or reefs originally deposited horizontally under water (Vermeulen, 2001). Subsequent overburden and geological movements transformed the reefs into tilted or faulted strata with an average thickness of 300 mm. Generally the reefs exist in the form of coarse conglomerates, or less often, as greyish metamorphosed sedimentary rock. The conglomerates are composed of rock pebbles derived from vein quartz, quartzite, chert jasper or quartz porphyry cemented in a silicate matrix. In *Table 2-1*, Stanley (1987) summarizes the mineralogical composition of a typical gold reef in the Witwatersrand area.

| **Mineral** | **Abundance** |
|---|---|
| Quartz ($SiO_2$), primary and secondary | 70 – 90% |
| Muscovite and other phyllosilicates | 10 – 30% |
| Pyrites | 3 – 4% |
| Other sulphides | 1 – 2% |
| Grains of primary minerals | 1 – 2% |
| Uraniferous Kerogen | 1% |
| Gold | ~ 45 ppm in the Vaal reef |

*Table 2-1. Mineral composition of a typical Witwatersrand gold reef (Stanley, 1987)*

## 2.3 THE GOLD EXTRACTION PROCESS

Tailings can be defined as the by-product of the mining process, consisting of finely ground and chemically treated rock flour (Vermeulen, 2001). In order to understand how tailings behave, it is important to understand how tailings are produced. The extraction of gold from the gold-bearing rock requires many

stages. The ore is first removed from the gold-bearing reef by drilling and blasting, which is known as the ore-winning process. This is followed by the process of ore-dressing, which is the mechanical preparation of ore rocks by crushing and grinding to liberate and expose the concentrated valuable minerals for metallurgical extraction (Ritcey, 1989). The main objective of ore-dressing is to increase the surface area available for metallurgical extraction by reducing the size of the ore. The size of the resulting rock flour has a significant influence on the behaviour of the tailings. Ore-dressing is followed by metallurgical extraction in which ore-minerals are extracted chemically through the processes of amalgamation or cyanidation (Stanley, 1987). Finally, the extracted gold is upgraded at the refinery to at least 99.5% pure by either the miller chlorination process or electrolytic refining. A detailed description of the gold extraction process is presented by Vermeulen (2001).

According to Vermeulen (2001), the Witwatersrand gold reef has an average grade of 8.74g/t. This implies that 1 tonne of rock flour is produced for every 8.74g of gold produced. Ripley et al. (1982) suggested that approximately 5 tonnes of solid and liquid waste is produced for every 10g of gold produced. The amount of tailings produced in the world was approximately 5 billion tonnes per year in 1994 (Vermeulen, 2001), and according to Penman (1994), this amount exceeds the amount of fill in the construction of embankment dams, motorway embankments and all other earthworks in the same period. In 1987, South African mines were producing in excess of 250 million tonnes of mine tailings annually. With such an amount of waste produced, it is not surprising that tailings impoundments were described by Smith (1972) as ‘massive manhills’. These massive structures pose great risk to the public and the environment in the event of a failure.

## 2.4 TAILINGS DISPOSAL

As a significant amount of tailings are produced, the environmental impact of this waste material can be of great concern. The disposal site and method is

dependent on factors such as capital and operating costs, experience and preference, site topography and climate conditions (Vermeulen, 2001). Mining waste was traditionally dumped into the nearest water body. Such disposal methods have been eliminated due to an increase in environmental awareness. Tailings nowadays are generally disposed of into impoundments specially designed for storage and containment of the solid and liquid waste.

### 2.4.1 Tailings deposition methods

Deposition of tailings into an impoundment can either be dry, sub-aqueous or sub-aerial slurry, or in a dewatered slurry state. However, due to the financial implications of transportation and placement, initially dry tailings are usually slurried prior to disposal. Tailings slurry is usually pumped at the highest concentration feasible to reduce the cost of transportation and placement. The following section briefly describes the depositional methods that are commonly used in practice.

**Dry deposition**

As the name suggests, tailings in a dry state are deposited without the addition of water. This is usually in the form of ash produced from thermal coal-fired power stations, or the coarse rejects from some coal, metal or mineral recovery process (Robertson, 1987). Placement and handling of dry tailings is essentially similar to any other earth or overburden moving exercises. Essentially, dry tailings differ from slurried tailings in two fundamental aspects. Firstly, interim stability is usually of less concern and a retaining embankment is usually not required. Secondly, the tailings are usually of sufficient strength for compaction equipment to be used during placement.

**Dewatered tailings**

Tailings within this category may range from a sloppy semi-slurry to a product which behaves essentially as a dry granular material (Robertson, 1987). The ‘handleability’, ‘trafficability’ and stability of the deposit are essentially dependent on the degree of dewatering achieved. Sloppy semi-slurry cannot provide a trafficable surface and deposition requires specialized placement

equipment such as conveyors while 'dry' dewatered tailings can be deposited and compacted by conventional earth-moving equipment.

The only significant difference between sloppy dewatered tailings and slurry placed tailings is the uniformity (lack of segregation) that results from dewatered deposits. 'Dry' tailings are placed in a partially saturated state and can be compacted to achieve the desired densities, consolidation or shear strength characteristics (Robertson, 1987).

Due to the financial implications of tailings transportation, it is common practice to pump tailings as slurry to the disposal site. This might not be feasible in areas where evaporation occurs at a fast rate or the use of water needs to be minimized for cost implications. In such cases, tailings can be placed dry or in a dewatered state. Although these methods can be implemented at reduced water consumptions, other equipments are required for the facility, which increases the capital and operational costs.

**Sub-aqueous deposition**

Sub-aqueous deposition usually involves deposition of slurry in an uncontrolled manner into a body of water. Tailings settle out as soft-bottom sediment, or are transported and dispersed over a large area under water (Vermeulen, 2001). The resulting low density material is generally very soft and may require special construction techniques and reclamation procedures.

Sub-aqueous deposition generally results in tailings with fairly uniform grading. Deposition under water results in a low density material that is generally normally or under-consolidated. These deposits can generally be characterized by a high void ratio, high compressibility and a low permeability (Robertson, 1987).

**Sub-aerial deposition**

Sub-aerial deposition generally involves deposition of slurry in an aerial manner, usually in the form of open-ended pipe discharge, spigotting or cycloning.

- *Open-ended pipe discharge*: This method is often used as an inexpensive delivery system, typically accomplished by discharging the slurry from one or more open-ended pipe outlets around the perimeter of a dam. Discharge sequence is cycled around the dam perimeter to allow the recently deposited slurry sufficient time to dry and gain strength before the next layer is placed. The slurry exiting the pipe outlet forms a plunge pool from which it breaches and flows towards the central semi-permanent pond. Flow is fast and concentrated on the beach (sloped area above water level) before fanning out in a delta towards the pond area. Ideally, segregation should take place on the beach, leaving coarse particles closer to the daywall and finer material in the central area. Although there is a general trend of fineness towards the pond, flow on the beach tends to concentrate in meandering streams of high velocity, passing most of the material directly into the pond, leaving little opportunity for segregation (Penman, 1994).

- *Spigotting*: Very similar to open-ended pipe discharge, but with the objective of reducing the velocity of the deposited stream and encouraging sheet-like flow across the beach to aid segregation (Vermeulen, 2001). This is accomplished by partially covering the delivery pipe outlet with a faceplate, leaving only a half moon opening. The slurry is sprayed over a large area on the beach with more uniform sheet-like flow. This form of deposition effectively separates the coarse fractions from the fines by gravitational segregation on the beach, and is generally used for tailings that have a wide grading and a high percentage of clay-sized particles. Deposition is achieved by groups of 20 to 40 spigots, placed at 1 to 5 metre intervals, which have to be raised periodically as the dam rises.

- *Cycloning:* The slurry can be cycloned to mechanically separate the slurry into the coarse fractions (cyclone underflow) and the finer material (cyclone overflow). The relatively free-draining characteristic of the coarse fraction makes it a suitable construction material, as it is relatively uniform in terms of particle size, consolidates rapidly, and produces a low water

table (Robertson, 1987). The finer overflow fraction is deposited by conventional spigotting techniques at a low slurry density. Operation of a cycloning system requires planning and management in order for the dam to function properly. It is only practical when the tailings have a wide grading and sufficient coarse fraction for daywall construction (Vermeulen, 2001).

### 2.4.2 Tailings dam construction methods

There are essentially three primary types of disposal facilities. Disposal of tailings can be done in natural basins such as under-sea or in-lake disposal as practiced in Canada and New Guinea (Robertson, 1987) or in-pit disposal. Although these methods minimize financial implications, environmental damage from under-sea or in-lake disposal can potentially be catastrophic.

Disposal can also be done as a central discharge cone deposit, commonly known as thickened discharge method (Robrinski, 1975). No embankments are required and deposition is achieved from a central discharge point onto the surface of the ground. The most critical factor is the angle of beach slope, as this determines the area and volume of the deposition cone (Robertson, 1987). The slurry is often thickened to increase the beach angles and thus the storage capacity of the cone.

The third method, which is the most common method of tailings disposal, involves construction of an embankment. Construction can be done in a valley such as conventional earth or rock filled dam construction methods or as freestanding raised embankments. Raised embankments are frequently used for tailings dam construction due to the flat terrain. There are three methods of construction for raised embankments, namely upstream, downstream or centreline construction.

**Upstream construction**

This method involves advancing the impoundment crest upstream by periodically constructing small dykes on the tailings deposit immediately

upstream from the previous deposition. The upstream method is shown in *Figure 2-1*. The main concern with upstream construction is that the successive dykes are constructed on previously deposited material and this requires that the deposited tailings have sufficient shear strength for stability. This method of construction should be avoided in regions of seismic activity.

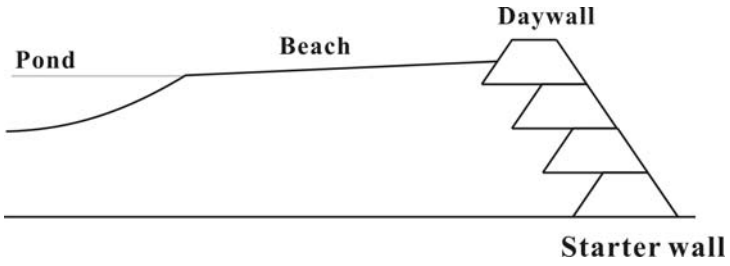


*Figure 2-1. Upstream method of tailings dam construction*

**Downstream construction**

Downstream construction is achieved by advancing the crest downstream as the smaller dykes are constructed. This is illustrated in *Figure 2-2*. The method is only required when the tailings are extremely weak, where the pool is impounded against the embankment, or in areas of severe climatic, seismic or toxic conditions. Additional area and thus cost are required for this type of construction (Robertson, 1987).

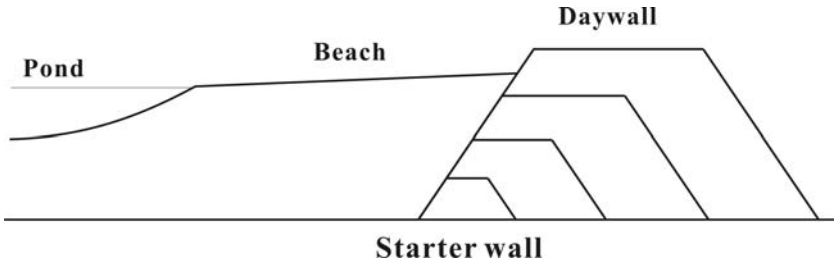


*Figure 2-2. Downstream method of tailings dam construction*

**Centreline construction**

With this method the crest is raised vertically upward as illustrated in *Figure 2-3*. Successive smaller dykes are constructed on the upstream side on previously deposited material and on the downstream side on borrowed or cycloned material over which some control can be exercised. The method is a balance between upstream and downstream construction methods.

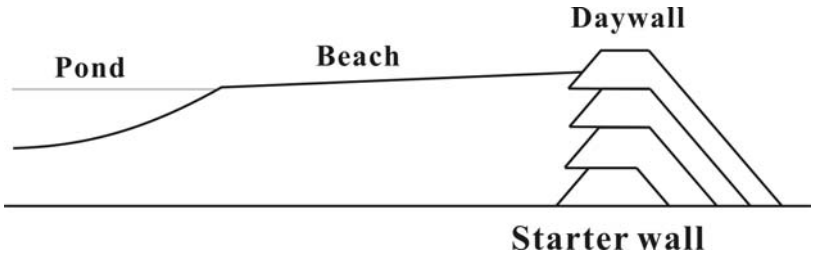


*Figure 2-3. Centreline method of tailings dam construction*

**Daywall-Nightpan Paddock system**

The method can be used in conjunction with upstream, downstream or centreline construction aforementioned. The periphery, also known as the daywall, is sectioned into paddocks in which tailings are poured from the midpoint. The fill is then compacted, either by tractor plough, or by labour intensive shovel packing. Excess water is decanted into the interior of the dam known as the nightpan. The daywall is left to dry, consolidate and crack for up to three weeks before the next lift, improving the mechanical properties of the material as a result of densification (Blight and Steffen, 1979). The construction of the daywall is entirely done during the day, due to the required supervision and close control, and hence the name. During the night, tailings are discharged into the interior or nightpan.

Paddock systems are successful when the tailings of fairly uniform grading remain well in suspension at a constant density until placed, and when the rate of rise matches the drying time of the tailings (Gowen and Williamson, 1987). The method results in a reasonably firm and well consolidated daywall, while the material in the nightpan, especially in the pond area, are usually significantly less consolidated and soft (Wagener and Jacobsz, 1999).

The choice of deposition and construction method depends on site availability and type of material available for construction. The most common method of tailings disposal in South Africa is the construction of raised embankments in which tailings, generally in the form of slurry, can be stored. These impoundments are often high and pose great threat to the environment in the event of failure. The gradation, and thus permeability of the tailings, is largely a function of the method of deposition into the impoundment. The stability of

these impoundments is largely dependent on the position of the phreatic surface which is a function of the permeability of the tailings.

## 2.5 ENGINEERING PROPERTIES OF GOLD TAILINGS

The construction of tailings impoundments resembles that of a natural deposit. Transportation of sediments is followed by deposition, sedimentation and eventually consolidation due to self-weight or external loading (Imai, 1981; Schiffman et al., 1988). Tailings, however, have a very recent stress history compared with natural deposits (Vermeulen, 2001). The following sections deal with the formation and state of tailings in general and briefly discuss the fundamental particle properties, index parameters, particle size distribution and beach profile. Engineering properties such as permeability, compressibility and consolidation, stiffness, shear strength and void ratio are also considered. For a more detailed discussion on the state and composition of gold tailings, refer to Vermeulen (2001).

### 2.5.1 Tailings in general

After deposition, the slurry flows along the beach towards the pond, during which tailings particles are deposited. Coarse particles are deposited first, closer to the discharge point, while finer particles are deposited further away from the point of discharge. This is known as segregation or hydraulic sorting of tailings. The result is a decrease in particle size towards the pond and a beach sloping down towards the centre of the dam (Papageorgiou, 2004). Hydraulic sorting is one of the main factors influencing the in situ properties of gold tailings. The particle size distribution determines geotechnical parameters such as density, permeability and shear strength. These in turn influence the rate of drainage, consolidation characteristics, acceptable rate of construction, safe slope angle of daywall and maximum height (volume) of the tailings dam (Papageorgiou, 2004). One of the design objectives for a tailings dam is to promote hydraulic sorting, as coarser material deposited near the edge has higher shear strength and permeability.

Another consistent feature of tailings impoundments is the highly layered nature of the profile. Deposition generally takes place cyclically around the dam to allow sufficient time for the newly deposited material to desiccate and consolidate. This significantly increases the strength and storage capacity of the impoundment. Layers can vary between 10 to 200mm in thickness, and often take the form of alternating coarse and fine deposits, with up to 50% variation in fineness (Vermeulen, 2001).

### 2.5.2 Fundamental properties and index parameters

Unless any significant chemically reactions have taken place during chemical extraction, tailings solids basically has the same mineralogy as the parent rock from which mining took place. Energy dispersive X-ray spectrometry in the SEM showed that tailings consist mainly of silicon with varying amounts of sodium, aluminium, potassium, iron and sulphur. Mineralogy of typical tailings from the Witwatersrand gold reef can be summarized as 75% quartz, 10% muscovite, 5% pyrophyllite, 5% illite and small percentages of clinochlore, kaolinite and pyrite (Vermeulen, 2001). Gold tailings have been classified as fine, hard and angular rock flour, with 0 to 15% fine sand, 80 percent silt and 0 to 10% clay-sized particles slurried with process water (Vick, 1983; McPhail and Wagner, 1989). Specific gravity of gold tailings from the literature can be summarized in *Table 2-2.*

| **Reference** | $G_s$ |
|---|---|
| Pettibone and Kealy (1971) | 2.5 – 3.5 |
| Hamel and Gunderson (1973) | 3.1 |
| East et al. (1988) | 3.02 |
| Vermeulen (2001) | 2.75 |

*Table 2-2. Specific gravity, $G_s$, of gold tailings*

In terms of particle shape, gold tailings generally range from highly angular to sub-round to flat. Coarse tailings are composed of highly-angular to sub-

rounded particles with sharp edges and some rough surfaces (Mittle and Morgenstern, 1975; Lucia et al., 1981; Garga and McKay, 1984; Vermeulen, 2001). Fines consist mainly of flat plate-like particles and small amounts of bulky silt-sized particles (Vermeulen, 2001; Chang, 2004). Undispersed samples (*Figure 2-4*) show an aggregation of the finer plate-like particles around the bulky, coarse particles.

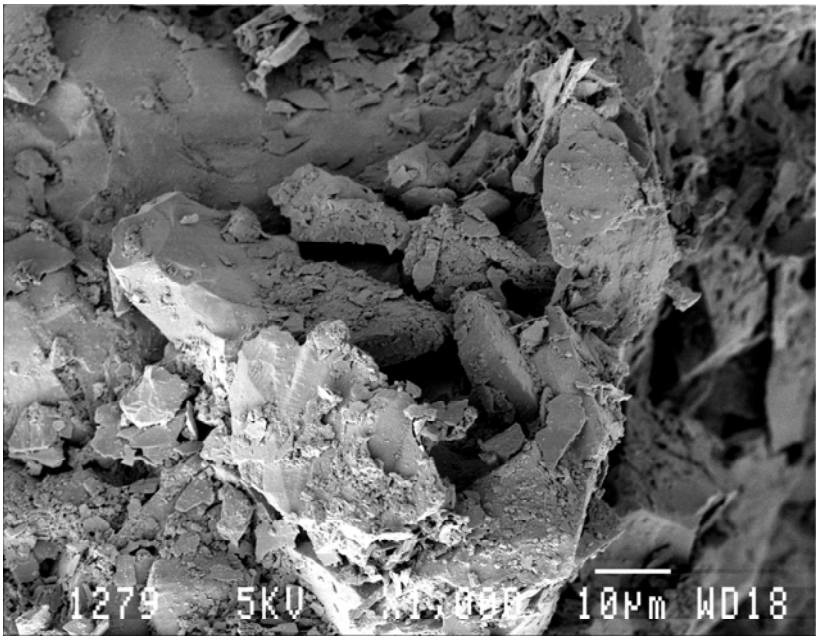


*Figure 2-4. Scanning electron micrograph of gold tailings (After Chang, 2004)*

Gold tailings generally exhibit little plasticity and no cohesion (McPhail and Wagner, 1989). Based on their Atterberg limits, gold tailings can be classified as low to high plasticity silts. The Atterberg limits of typical gold tailings from the Witwatersrand Gold reef are given in *Table 2-3* (Vermeulen, 2001):

| **Sample** | **Liquid limit** | **Plastic limit** | **Plasticity index** |
|---|---|---|---|
| | (%) | (%) | (%) |
| Whole tailings | 29 | 22 | 7 |
| Coarse (> 0.075mm) | 28 | 22 | 6 |
| Fines (< 0.075mm) | 43 – 56 | 32 – 39 | 11 – 17 |

*Table 2-3. Atterberg limits of typical gold tailings (Vermeulen, 2001).*

### 2.5.3 Particle size distribution

The grading or particle size distribution of gold tailings is a function of factors, such as, the effectiveness of the size reduction process, and the solid content of the slurry. Due to hydraulic sorting, the sampling position also has an effect on the grading of the gold tailings. Pettibone and Kealy (1971) and van Zyl (1993) described the grading of typical gold tailings as uniformly distributed in the silt size range with small percentages, in the order of 10 percent, in the sand and clay size ranges. *Figure 2-5* shows the grading envelope for typical South African gold tailings published by Blight and Steffen (1979).

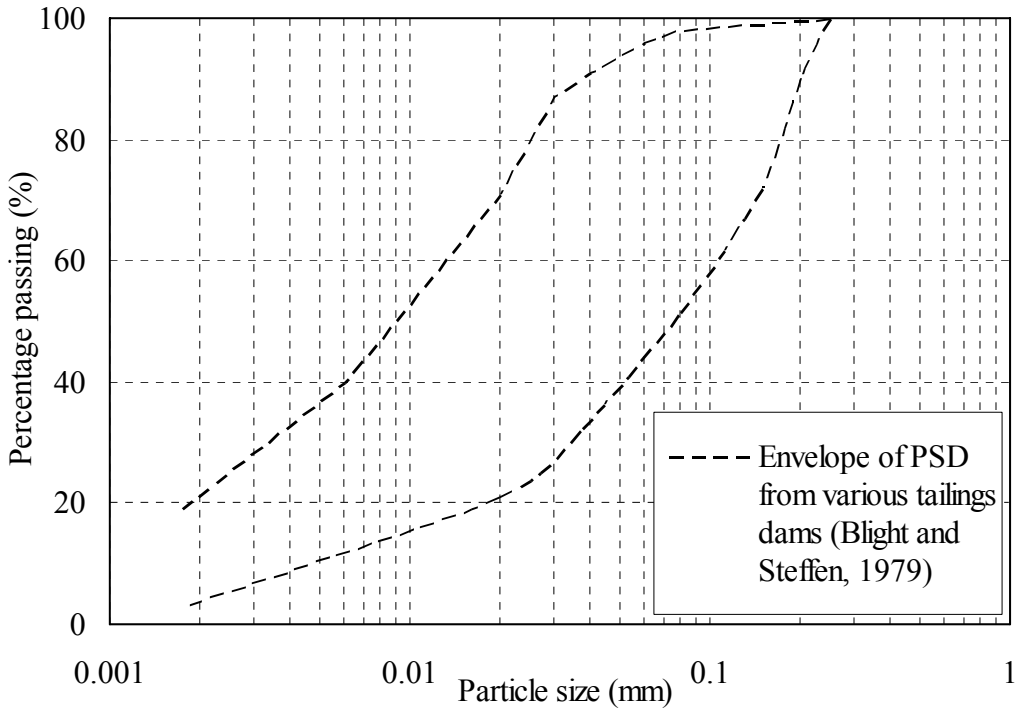


*Figure 2-5. Particle size distribution envelope of South African gold tailings (After Blight and Steffen, 1979)*

Vermeulen (2001) showed that after chemical treatment, which included removal of organic material and calcareous content and dispersion, grading properties could be summarized as in *Table 2-4*.

| Description | $D_{10}$ | $D_{30}$ | $D_{60}$ | $D_{90}$ | $C_U$* | $C_Z$** |
|---|---|---|---|---|---|---|
| | (µm) | (µm) | (µm) | (µm) | | |
| Whole tailings | 2 | 10 | 55 | 125 | 27.5 | 0.91 |
| Coarse (>0.075mm) | 2–3 | 9-25 | 43-75 | 115-145 | 21.5-25 | 0.94-2.78 |
| Fine (<0.075mm) | 1.5-1.7 | 3.2-4.5 | 8.3-16 | 41-55 | 4.9-10.7 | 0.75-0.84 |

*$C_U$ = Coefficient of Uniformity = $D_{60}/ D_{10}$

** $C_Z$ = Coefficient of Curvature = $D_{30}^2/(D_{10}D_{60})$

*Table 2-4. Summary of grading properties of dispersed gold tailings (Vermeulen, 2001)*

### 2.5.4 Permeability

The permeability of soil is a function of the particle characteristics, density and particle arrangement of the soil (Pettibone and Kealy, 1971). As a result of hydraulic sorting, tailings differ in grading, and thus permeability, from the peripheral wall to the pond. According to Kealy and Busch (1979), this variation in permeability is by far the most significant factor in determining the position of the phreatic surface. Anisotropy in permeability due to deposition cycles has significantly lesser effects on the location of the phreatic surface (Vermeulen, 2001). Quoted values for the permeability of gold tailings are summarized in *Table 2-5*.

| Reference | Description | Permeability (m/yr) |
|---|---|---|
| Blight (1980) | Range | 1 – 50 |
| Blight (1981) | General | 3 |
| Vermeulen (2001) | Whole tailings | 10 |
| | Fines | 1.5 – 5 |
| | Coarse | 2.5 – 15 |

*Table 2-5. Summary of permeability of gold tailings*

The permeability of the tailings material at any point down a slurry deposited beach can also be estimated by equations of the type:

$$k = ae^{-bH} \qquad \textit{Equation 2-1}$$

where $k$ is the permeability at a distance $H$ down the beach and $a$ and $b$ are constants of a particular beach and tailings. Blight et al. (1985) showed, using model beaches, that for a particular active gold tailings beach, $a$ = 2.72 x $10^{-5}$ m/s and $b$ = 0.0315 /m. The permeability can also be estimated via the well-known Hazen expression or by the expression given more recently by Sherard et al. (1984):

$$k = 0.35(D_{15})^2 \qquad \textit{Equation 2-2}$$

### 2.5.5 Compressibility and consolidation characteristics

Consolidation can generally be classified into primary and secondary consolidation. Primary consolidation deals with the gradual reduction in volume of a fully saturated soil as the excess pore water pressure, built up by an increase in total stress, dissipates. Secondary compression or creep, however, is thought to be due to the gradual realignment of particles into a more stable configuration with time under constant stress conditions. Primary consolidation can be expressed in terms of the *compression index* $C_c$, a measure of the stiffness of the material and in terms of the *coefficient of consolidation* $C_v$, which is an indication of the rate of consolidation. The value of $C_v$ can be determined using Casagrande's log-time method or Taylor's root-time method and the compression index $C_c$ is the slope of the linear portion of the *e*-log*p*' plot.

Tailings are generally more compressible than similar natural soils due mainly to their grading characteristics, high angularity and loose depositional state (Vick, 1983). Matyas et al. (1984) conducted oedometer tests on uranium tailings and found that fine tailings appear more compressible than coarse

tailings. Similar results were reported by Vermeulen (2001). Interestingly, Matyas et al. (1984) also concluded that the compressibility of undisturbed samples was higher than its reconstituted counterparts. *Table 2-6* shows typical values of $C_c$ for gold tailings as quoted in the literature.

| **Reference** | **Compression Index, $C_c$** | |
|---|---|---|
| | **Coarse** | **Fine** |
| Blight and Steffen (1979) | | 0.35 |
| Vick (1990) | 0.05 – 0.1 | 0.23 – 0.3 |
| Stone et al. (1994) | | 0.75 (centrifuge) |
| | | 0.35 (Rowe cell) |
| Qiu and Sego (2001) | | 0.083 – 0.156 |

*Table 2-6. Quoted values of Compression Index, $C_c$, for gold tailings*

The coefficient of consolidation for gold tailings reported in the literature is summarized in *Table 2-7*.

| **Reference** | **Coefficient of consolidation, $C_v$ (m²/yr)** | |
|---|---|---|
| | **Coarse** | **Fine** |
| Blight and Steffen (1979) | | 198 |
| Vick (1990) | $1.6x10^3 – 0.6x10^6$ | 0.3 – 30 |
| Stone et al. (1994) | | 15 – 26 |
| Vermeulen (2001) | 800 – 6900 | 210 – 1200 |
| Qiu and Sego (2001) | | 13.58 – 80.07 |

*Table 2-7. Coefficient of consolidation, Cv, for gold tailings.*

Very little literature was found dealing with creep of gold tailings, but according to Vick (1983), secondary consolidation in gold tailings is relatively insignificant compared to primary consolidation.

### 2.5.6 Stiffness

The bulk stiffness of a soil can be expressed by the *Bulk modulus, K*, as in *Equation 2-3*:

$$\frac{1}{K} = \frac{\delta p'}{\delta \varepsilon v} \qquad \textit{Equation 2-3}$$

where $\delta p'$ is the change in normal effective stress and $\delta \varepsilon_v$ is the change in volumetric strain. Isotropic compression tests data (Vermeulen, 2001) on reconstituted and undisturbed gold tailings samples is plotted in terms of the bulk modulus *K* and shown in *Figure 2-6*.

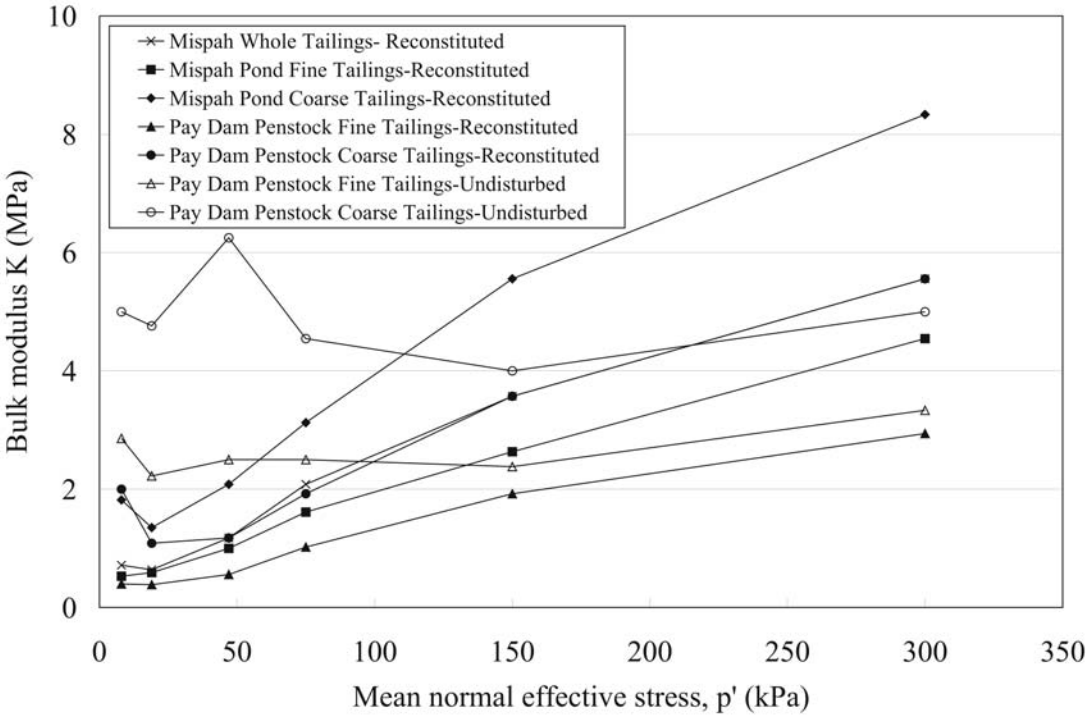


*Figure 2-6. Bulk modulus of undisturbed and reconstituted gold tailings samples.*

It is evident that fine tailings generally have a lower bulk modulus than coarse tailings. Furthermore, it is interesting to note that undisturbed samples have higher *K* values than their reconstituted counterparts.

The small strain stiffness of soils depends on the void ratio and the effective confining stress. $G_{max}$ for gold tailings was estimated from the bender element results (Chang, 2004) to be in the range of 20 to 200MPa for effective confining stresses of up to 400kPa. Höeg et al. (2000) assessed the small strain stiffness, $G_{max}$, of fine tailings of the Polish Zelazny dam, and found that the recorded $G_{max}$ of undisturbed samples were 20 to 30 percent higher than their reconstituted counterparts at the same state. The difference was attributed to soil fabric, as no evidence of cementation was found. Furthermore, $G_{max}$ seemed to decrease with increasing fines content.

### 2.5.7 Shear behaviour

The static shear strength of saturated soil can be expressed in terms of the effective angle of internal friction, $\varphi'$, and cohesion, $c'$. Gold tailings can be described as cohesionless in most cases, and having an effective angle of internal friction in the range of 30º to 37 º (Vick, 1983). According to Vick (1983), factors such as grading, density and over-consolidation ratio have a relatively small effect on $\varphi'$. The effective angle of internal friction is mainly dependent upon the effective stress level, with the strength envelope curved at high stresses due to particle crushing. The shear strength parameters of gold tailings in the literature are summarized in *Table 2-8*.

| **Reference** | **Material** | **Test** | ***c'* (kPa)** | ***φ'* (º)** |
|---|---|---|---|---|
| Hamel and Gunderson (1973) | Dense air-dry | Direct shear | 79 | 38 |
| | Loose air-dry | | 0 | 39 |
| | Loose wet | | 100 | 28 |
| | Dense, saturated | | 11 | 24 |
| Mittal and Morgenstern (1975) | Peak, loose | Direct shear | 0 | 34 |
| Blight and Steffen (1979) | Slimes | | 0 | 28-41 |
| Blight (1981) | General | | 0 | 35 |
| Vick (1983) | General | | | 30-37 |

| *Table continued…* | | | | |
|---|---|---|---|---|
| Sully (1985) | Average | Direct shear | 5 | 33 |
| Van Zyl (1993) | Sand/slimes | | 0 | 35 |
| Blight (1997) | Sand/slimes | Triaxial/ Direct shear | 0 | 29-35 |
| Vermeulen (2001) | Average | Triaxial | 0 | 34 |

*Table 2-8. Summary of static shear strength parameters of gold tailings quoted in the literature*

Vermeulen (2001) demonstrated, using both tube samples and moist tamped samples, that the stress paths generally show some phase transformation, and are seldom purely contractive or dilative. Theron (2004) reproduced the behaviour of gold tailings with a sand-mica mixture, and postulated that the mechanical behaviour of gold tailings is governed by the platy particles.

### 2.5.8 Liquefaction potential

According to Castro and Poulos (1977) and Sladen et al. (1985), liquefaction is defined as *a phenomenon wherein a saturated material loses a large percentage of its shear resistance (due to monotonic or cyclic loading) and flows in a manner resembling a liquid until the shear stresses acting on the mass are as low as its reduced shear resistance*.

The behaviour of soils may be described as strain-hardening or strain-softening and as contractive or dilative.

- *Strain-hardening*: plastic straining beyond the yield point is accompanied by increase in stress.

- *Strain-softening*: plastic straining beyond the yield point is accompanied by a decrease in stress.
- *Contraction*: loading of loosely packed particles results in a tendency for a decrease in void space. Under undrained conditions, this leads to an increase in pore pressure and a resultant decrease in effective stress. Contraction is demonstrated using the marble analogy in *Figure 2-7a*.
- *Dilation*: loading of densely packed particles results in a tendency for an increase in void space. The resultant decrease in pore pressure leads to an increase in the effective stress. This is demonstrated in *Figure 2-7b*.

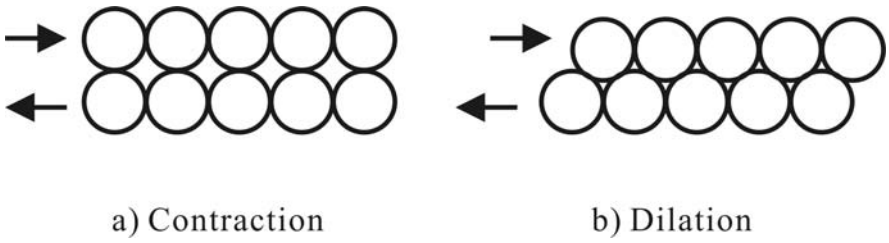


*Figure 2-7. Marble analogy demonstrating contractive and dilative behaviour.*

Saturated cohesionless soils may display one of three possible types of behaviour as displayed in *Figure 2-8* when subjected to undrained loading (Papageorgiou, 2004):

- *Contractive/liquefaction/strain-softening behaviour:* displays an increase in pore pressure to a constant value accompanied by a peak in the deviatoric stress within a few percent of loading followed by a sudden decrease to a constant residual value. The stress path moves to the left during the entire shear process, initially up (increase in *q'*) and then down after the peak has been reached. This is demonstrated in *Figure 2-8* curve *(a)*.
- *Dilative/strain hardening behaviour*: displays an initial increase followed by a continuous decrease in pore pressure. The deviatoric stress increases continuously throughout the shear process. This is demonstrated in *Figure 2-8* curve *(b)*.

- *Limited liquefaction*: defined as a soil which exhibits a temporary decrease followed by an increase in the shear strength as strain increases. Limited liquefaction is demonstrated by curve *(c)* in *Figure 2-8.*

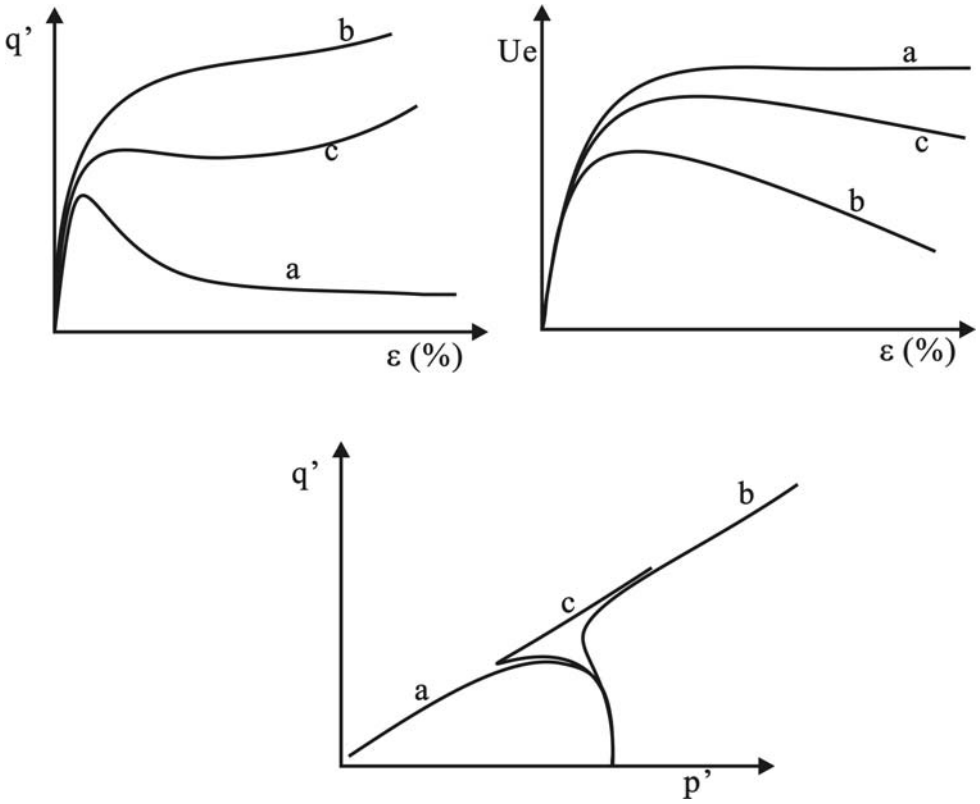


*Figure 2-8. Possible behaviours for saturated cohesionless soils.*

It has been shown by researchers such as Vaid et al. (1990) and Vaid and Sivathalayalan (2000) that moist tamping generally produces strain-softening behaviour while samples produced using water pluviation techniques generally dilate. It has also been concluded by the Canadian Liquefaction Experiment (CANLEX) that samples produced using water pluviation techniques generally show better agreement with undisturbed samples of Syncrude sands.

The reduction in undrained strength of a strain-softening material may be expressed in terms of the brittleness index, $I_B$ (Bishop, 1967):

$$I_B = \frac{\sigma_{dp} - \sigma_{dr}}{\sigma_{dp}} \qquad \textit{Equation 2-4}$$

where $\sigma_{dp}$ is the peak undrained shear strength and $\sigma_{dr}$ is the residual undrained shear strength. The brittleness index ranges between 0 and 1, with a higher $I_B$ associated with a higher reduction in shear strength.

### 2.5.9 Density and void ratio

The density or void ratio of most natural deposits can be estimated by acquiring undisturbed samples. The difficulty in estimating the density state of mine tailings arises from the inability to obtain undisturbed samples, especially in the pond area. Vermeulen (2001) suggested that, depending on

| Reference | Description | Density (kg/m³) | Void ratio |
|---|---|---|---|
| Blight (1969) | After deposition | | 1.7 |
| | After evaporation | | 1.25 |
| | After sun drying | | 0.5 |
| Blight and Steffen (1979) | General | | 1.1-1.2 |
| Blight (1981) | In situ dry density | 1835 | |
| Vick (1983) | Tailings sand | | 0.6-0.9 |
| | Low plasticity slimes | | 0.7-1.3 |
| | High plasticity slimes | | 5-10 |
| East et al. (1988) | In situ dry density | 1340-1740 | |
| | Average dry density | 1650 | |
| van Zyl (1993) | In situ dry density | 1000-1450 | |
| Vermeulen (2001) | Delivery pulp dry density | 300-750 | |
| | In situ dry density (sands) | 1250-1650 | |
| | In situ dry density (slimes) | 1000 | |
| | In situ void ratio (coarse) | | 0.77-0.87 |
| | In situ void ratio (fine) | | 1.39-1.49 |

*Table 2-9. In situ densities and void ratios for gold tailings*

the specific gravity, pond tailings settle to a dry density of approximately 1000kg/m³ with a moisture content of 60 percent while on the beach tailings generally settle to a density of approximately 1450kg/m³ with a moisture content of 20 to 50 percent. Furthermore, density increases with depth as consolidation takes place. Vick (1983), however, suggests that the in situ void ratio of tailings is a better indication of the density state than dry density, as void ratio excludes the effects of specific gravity and is only a function of tailings particle properties and stress level. In situ densities and void ratios are summarized in *Table 2-9*. In situ void ratio is also dependent upon the grading of the tailings. Coarse particles close to the daywall settle to a lower void ratio than finer material further down the beach or in the pond (Vermeulen, 2001).

## 2.6 SOIL FABRIC

The effect of particle arrangement has long been recognized, even in the early days of soil mechanics development, with little or no substantial evidence. In the mid-1950s, with the development of suitable optical, X-ray and electron microscopes, direct observations became possible. Interest was mainly centred around clay particle arrangement and their effects on mechanical properties. In the late 1960s, improved techniques of sample preparation and the development of the scanning electron microscope (SEM) greatly facilitated the expansion of the science. In the early 1970s research interest expanded to include cohesionless soils and this led to the realization that soil characterization cannot be done in terms of density or relative density alone. Soil behaviour is also dependent upon stress history and the soil structure (Mitchell, 1993).

### 2.6.1 Observed difference in behaviour of soils

It is generally agreed that the fabric of clays may affect the behaviour of the clay (e.g. Seed et al., 1962; Mitchell, 1993). Various researchers have also demonstrated that cohesionless soils prepared using different reconstitution methods display different behaviour:

- Based on results of cyclic triaxial tests performed by Mulilis et al. (1977), Ishihara (1993) showed that the resistance to liquefaction of samples from the same type of sand prepared at the same relative density can vary over a wide range depending on the nature of the fabric created by different methods of sample preparation.
- Seed and de Alba (1986) and Yoshimi et al. (1989) showed that both the shear strength and liquefaction resistance of soils in its natural, undisturbed state are found to be significantly larger than measured in the laboratory.
- Zlatovic and Ishihara (1997) demonstrated that sand prepared using different reconstitution methods to similar void ratios (0.799 and 0.802) behaves differently under the same stress conditions. Water pluviated samples show strain-hardening behaviour while moist tamped and dry deposited samples show temporary strain-softening.
- Vaid et al. (1999) showed that the undrained response of uniform medium-grained sand could exhibit different undrained response at the same void ratio and effective stress conditions. Loose sand, when moist tamped, is contractive and susceptible to liquefaction while water pluviated specimens show dilative behaviour. This contractive, strain-softening response is due to the loose, collapsible structure that ensues upon moist tamping. They further concluded that characterizing in situ fluvial deposit and hydraulic fill sands using moist tamping will unjustifiably condemn it as being liquefiable.
- Wood (1999) showed that the specimen reconstitution method could influence the liquefaction behaviour of the silty sand. Dense and loose specimens formed from various reconstitution methods show similar behaviour: dense silty sand exhibits dilative behaviour and loose material shows contractive behaviour. The undrained response of medium silty sand can, however, be profoundly influenced by the reconstitution method. In general, wet methods are more resistant to liquefaction.

Although it is commonly believed that the difference in observed behaviour is a result of different fabric, there has however been a lack of substantiating evidence. Researchers have generally observed differences in behaviour

between in situ samples and samples reconstituted using various methods and speculated that the difference in behaviour is a result of fabric differences. In the past two decades, with the aid of improved image analysis methods and availability of microscopy equipment, fabric analysis is becoming increasingly feasible. If the fabric does indeed affect the behaviour of cohesionless soils then it is important to incorporate the effect of fabric in the soil models.

### 2.6.2 Description of soil fabric and fabric elements

Fabric description has traditionally been used by soil scientists to facilitate their understanding of root growth and fluid movement. It is, however, becoming increasingly used in the description of soils for geotechnical research. The fabric of soils can, in general, be described as comprising three distinct elements (Collins and McGown, 1974). This is demonstrated in *Figure 2-9.* Natural soils are generally composed of one or some of these fabric features:

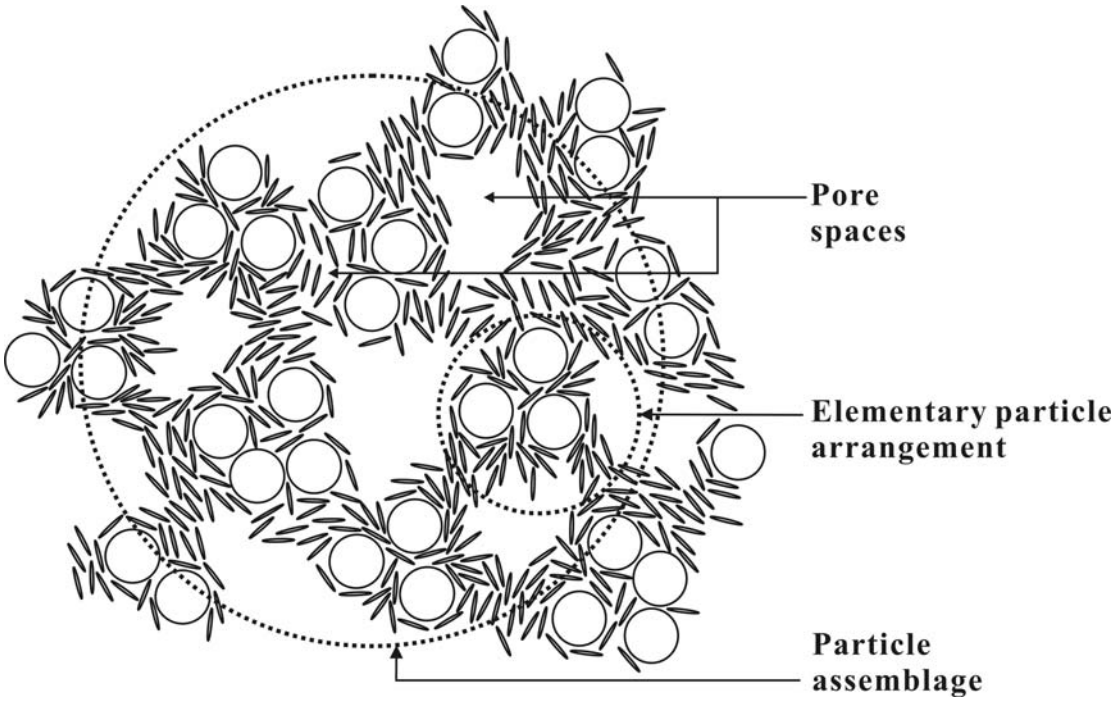


*Figure 2-9. Three distinct elements of soil fabric.*

- *Elementary particle arrangements:* single forms of particle interaction at the level of individual clay silt or sand particles.
- *Particle assemblages*: units of particle organization having definable physical boundaries and a specific mechanical function, which consist of one or more forms of the elementary particle arrangement.
- *Pore spaces*.

The fabric of a soil may also be considered, based on the level of scale (Mitchell and Soga, 2005):

- *Micro-fabric*: consists of the regular aggregation of particle and the very small pores between them. Typical fabric units are up to a few tens of micrometres across.
- *Mini-fabric*: contains the aggregation of the micro-fabric and the inter-assemblage pores between them. Mini-fabric units may be a few hundred micrometres in size.
- *Macro-fabric*: contains cracks, fissures, root-holes, laminations etc that correspond to the trans-assemblage pores.

Mechanical and flow properties of soils depend, to a varying degree, on these three levels of fabric. Hydraulic conductivity will be a function of the macro- and mini-fabrics while creep will be dependent on mini- and micro-fabrics (Mitchell, 1993).

### 2.6.3 Methods of fabric measurement

Various methods have been used to analyse the fabric of soils. These techniques range from visually observing the fabric under a microscope to measuring the electrical conductivity (Anandarajah and Kuganenthira, 1995) of the soil. The methods give insight into the observed behaviour of the soil through the fabric. These methods can be categorized into indirect and visual methods, which are summarized with example references in *Table 2-10*.

| METHOD | REFERENCE |
|---|---|
| **Indirect methods** | |
| Mercury intrusion porosimetry (MIP) | Lefebvre and Delage (1983) |
| Hydraulic conductivity | Dewhurst et al. (1996) |
| Wave velocity | Pan and Dong (1999), Santamarina and Cascanta (1996) |
| Electrical conductivity | Anandarajah and Kuganenthira (1995) |
| **Visual methods** | |
| Optical Microscopy | Oda and Kazama (1998) |
| Thin sections | Oda and Kazama (1998) |
| Scanning Electron Microscopy (SEM) | Cafaro and Cotecchia (2001), Cotecchia and Chandler (1997), Fearon and Coop (2000) |
| X-ray computed tomography | Oda et al. (2004) |
| Laser scanning confocal microscopy | Fredrich et al. (1995) |

*Table 2-10. Indirect and visual methods for fabric analysis*

Visual methods involve collecting and analyzing image data while indirect methods involve measuring some physical quantity and relating them to the fabric of the material. Other available visual methods used in soil testing that have not been referenced are x-ray scattering, neutron scattering and nuclear magnetic resonance. These methods require investigation regarding their suitability for soil fabric analysis, but provide potential possibilities.

This section deals with the various methods available for measurement and analysis of fabric, and includes the basic principles, benefit and limitations of each method.

**Indirect methods**

These methods are used to give an idea of the arrangement of the particles without visually observing the particles. Indirect methods measure various

properties of the material and relate the properties to the arrangement of the particles. Indirect methods (except for MIP) are generally used to assess fabric anisotropy.

- *Mercury intrusion porosimetry (MIP)*: This method is based on the principle that a non-wetting fluid, like mercury, does not enter a porous medium unless sufficient pressure is applied to force the liquid into the pores. Assuming pores to be cylindrical capillaries, the pressure, $P$, is related to the entrance pore radius, $r$, by Laplace's Law:

$$P = \frac{2\sigma \cos\theta}{r} \qquad \textit{Equation 2-4}$$

  where $\sigma$ is the surface tension of the intruding liquid and $\theta$ is the contact angle (for mercury, $\sigma$ = 0.484 N/m and $\theta$ = 141°). By increasing $P$, increasingly smaller pores are filled and the results can be plotted on a cumulative curve giving the pore-size distribution of the porous medium. The benefit of this method is that it is non-destructive (Lawrence, 1978) and does not cause damage the soil. There are a few limitations to the method. Firstly, the soil needs to be dehydrated before mercury intrusion can take place. However, air or oven drying may cause significant shrinkage of clays with high water content. Secondly, mercury intrusion porosimetry does not indicate the exact size of the pores, but rather the size of the entrance of the pores. Finally, the use of the method requires special care, since mercury is a poisonous substance.

- *Hydraulic conductivity*: The hydraulic conductivity of a material is a function of its fabric, thus development of an anisotropic fabric (Morgenstern and Tchalenko, 1967) may result in anisotropy in hydraulic conductivity (Arch and Maltman, 1990). Field and laboratory studies have suggested that shear zones in clays may enhance or retard fluid flow (Lupini et al., 1981). The behaviour of large strain shear zones is governed by the residual fabric of the sheared soil, which is dependent on the clay content and composition (Dewhurst et al., 1996). Hydraulic conductivity

may be used as a relative measure of fabric. By comparison of the hydraulic conductivity in two directions, the material anisotropy can be determined. The method, however, cannot yield a unique measure of fabric.

- Wave velocity: Particulate mechanics suggest that the mechanical behaviour of a particulate material is dependent on the distribution and orientation of the particles and the contact forces. Elastic wave velocity (including compression and shear waves) can be related to the fabric of granular material and its evolution during shearing (Santamarina and Cascanta, 1996; Pan and Dong, 1999). The fabric of a natural granular assembly can be evaluated from wave velocity measurements via an analytical procedure. This procedure involves a stress-dependent micromechanics-based elastic model, a theory of elastic-wave propagation for anisotropic material, and an optimization procedure (Pan and Dong, 1999). The analytical procedure is illustrated in *Figure 2-10.*

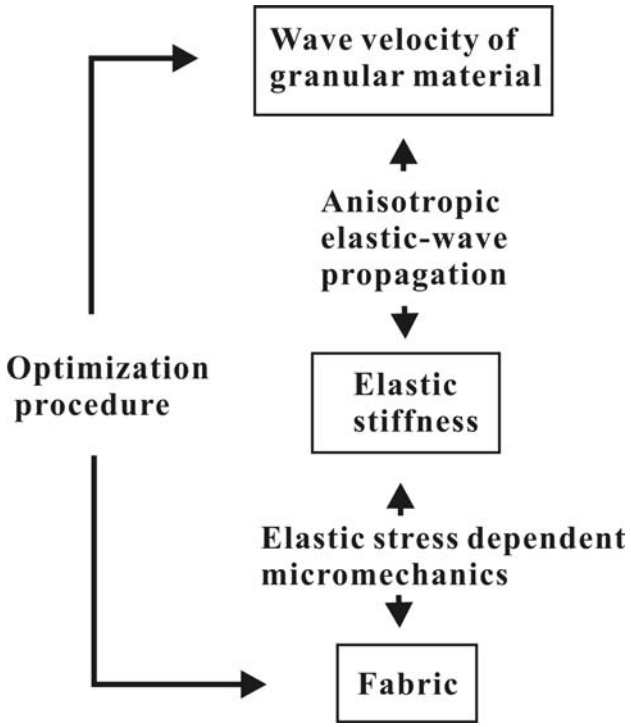


*Figure 2-10. Analytical procedure for determining the relationship between fabric and measured wave velocity (Pan and Dong, 1999).*

The analytical procedure relates wave velocity anisotropy to the anisotropic distribution of fabric and contact forces. The results indicate that an assembly shows a concentration of contact normals in the major principle direction and a residual fabric after subsequent loading/unloading sequences (Pan and Dong, 1999).

- Electrical conductivity: Electrical conductivity can be measured between two electrodes on either side of a saturated soil specimen, as shown in *Figure 2-11*. The soil skeleton is non-conductive, and thus electricity flows through the interstitial fluid. The conductivity of the specimen $\sigma$, can be defined as:

$$\sigma = L / RA \qquad \textit{Equation 2-5}$$

where $L$ is the length of the distance between the electrodes, $A$ is the area of each electrode and $R$ is the measured resistance. $\sigma$ is a function of the conductivity of the pore fluid $\sigma_f$, the void ratio, and the orientation of soil particles. The vertical path shown in *Figure 2-11* is more tortuous than the horizontal path, and so $\sigma_v$ will be less than $\sigma_h$. The magnitude of $\sigma_v$ and $\sigma_h$ will also depend on the value of $\sigma_f$.

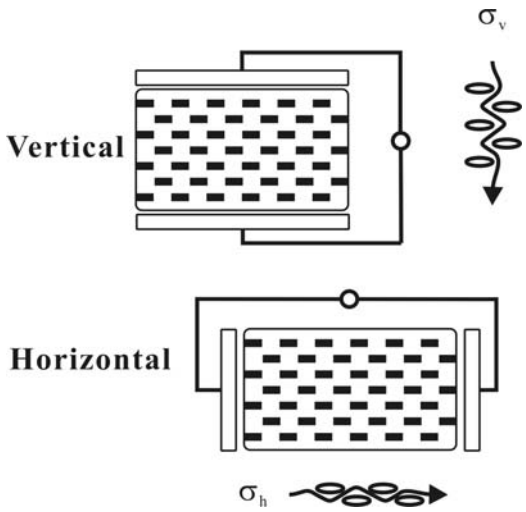


*Figure 2-11. Electrical conduction in clay specimen in vertical and horizontal directions (After Anandarajah and Kuganenthira, 1995).*

The major problem with most indirect methods is that the fabric is not visually observed and verified. The fabric is often related to the measured property by mathematical expressions or empirical relationships. The advantages are that firstly, the methods are usually non-destructive, and secondly, the measured properties can be expressed quantitatively as opposed to qualitatively. Measurements are also averages over the entire specimen and the possibility of measuring only the property of a specific structural feature is thus minimized.

**Visual methods**

The principles of all visual techniques involve bombarding the sample with particles, and monitoring the ejected particles. The methods are differentiated in terms of the types of incident and ejected particles. The ejected particles are then analysed and presented as an image from which the fabric can be visually observed and analysed.

- Optical microscopy: An object becomes visible when light is reflected off the object to an image capturing device, such as the human eye. When a lens is placed in between the object and the image capturing device, the refractive property of the lens changes the focal point of the light-rays, and the image can be magnified. The applications of optical microscopy are somewhat limited in geotechnical engineering. Firstly, the magnification that can be achieved with an optical microscope is limited due to properties of light (usually to a few hundred times magnification), and secondly, the clarity of images is restricted to the depth of focus of the lens. Other positions which do not fall within the depth of focus will seem blurred.

- Thin sections: Different elements can be identified by making use of the difference in refractive index between various crystal lattices which exist in different elements. The section must be sufficiently thin to allow passage of light-rays. Thin sections can be produced from soil specimens by impregnation with a suitable resin. Impregnated specimens are

sectioned and polished before they can be viewed. This method is an excellent way of observing grain orientations within a soil specimen.

- Scanning Electron Microscopy (SEM): This method has been used extensively in the geotechnical field for topographical imaging purposes (eg. Cotecchia and Chandler, 1997; Fearon and Coop, 2000; Cafaro and Cotecchia, 2001). The principle of SEM is to bombard the specimen with an incident electron beam, and to detect the emitted electrons. Two main types of electrons are emitted, namely secondary electrons and back-scattered electrons.

  Secondary electrons are emitted when incident electrons knock loosely bound conduction electrons out of the sample. The intensity of the signal is dependent upon the angle between the incident beam and the specimen surface. A strong signal (large amounts of emitted electrons) will produce a bright spot, and a weaker signal (small amounts of emitted electrons) will produce a darker spot. Back-scattered electrons may be emitted when an electron beam passes close to a positively charged atomic nucleus and is attracted by its positive charge. Depending on the electron energy and the distance away from the nucleus, the angle of electron deflection may vary between 0 to 180°. These deflected electrons are collected by the detector and an image is produced from these back-scattered electrons. Similar to secondary electron images, the brightness of the image is dependent on the amount of electrons detected at a particular position.

  The electron beam, typically with a radius of 5nm scans the specimen and an image is produced with bright or dark spots at the corresponding position. The images produced are three-dimensional topographical images with a shallow depth of view, because electrons cannot be detected from deep inside the specimen. The main difference between a back-scattered electron image and a secondary electron image is that a back-scattered electron image is a function of the atomic number while a secondary electron image is dependent upon the topography of the specimen.

Non-conductive specimens, like soil, need to be coated with a conductive coating to reduce electrical charging of the specimen, which creates image defects. This is usually accomplished with sputter-coating of gold or gold/palladium alloy. The use of a metal coating also yields a stronger signal and can aid in conducting heat and excess electrons away from the specimen.

SEM usually produces excellently clear images at very high magnifications. By varying the type of emitted electrons topographical or compositional images can be produced. There are a few limitations to SEM. Firstly the image is a three-dimensional surface image. When internal images of soil are required, it is necessary to open up the specimen which causes disturbance. Furthermore, the soil needs to be dry, as the sample is placed under high vacuum and any volatile material will cause contamination of the vacuum chamber leading to a reduced resolution.

Another benefit of SEM is its ability to produce x-rays which can be used to provide compositional information about the specimen. When an electron beam interacts with an element, an electron in the element may be removed, causing a vacancy. If the vacancy is at a higher energy, an electron from the outer shell (at lower energy) will fall into the vacancy. Energy is released in this process in the form of a photon of electromagnetic radiation. If the ejected electron was from an inner shell, then the photon is an x-ray. The released energy varies with the atomic number and can therefore be used to identify various elements.

- X-ray microscopy: X-radiation occurs when electrons, highly accelerated under high voltage, reduce speed when collided against a target made of a heavy metal such as tungsten. When an x-ray passes through an object, it attenuates at different rates, depending on the distribution of its electron density, if the x-ray energy level is kept constant (Johns et al., 1993). The attenuation of the x-ray is recorded on a detector and from the attenuation data, an image is created by means of a numerical technique known as *filter-back projection*. If the attenuation properties change sharply across

the material, it is possible to identify the boundaries of the material. The target, which corresponds to the x-ray source, must be small enough to minimize the scattering zones of the x-ray detector. A microfocus x-ray system uses a target as small as 5µm, and therefore the resolution of the image is greatly improved.

Oda et al. (2004) successfully imaged a sample of Toyoura sand ($D_{50}$ = 0.206mm) using a microfocus x-ray system to investigate the microstructure in the shear band of the sample after shear. Although the sand was impregnated with a resin before imaging, the procedure was not necessary. The advantage of microfocus x-ray computed tomography is that sample preparation and imaging is simple, and the images obtained are three-dimensional images. The problem is that the x-ray apparatus with a microfocus target is extremely expensive and scarce, and the clarity of the image is not as good as SEM images.

- Laser scanning confocal microscopy: Laser scanning confocal microscopy (LSCM) has been used extensively in the biological sciences, but has only limited applications with geological material such as soils and rocks. Light (laser) particles are used as incident particles and imaging is achieved from the reflected light particles. LSCM involves saturating the specimen with an epoxy mixed with a suitable fluorochrome. The natural weak fluorescence of minerals allows a contrast between the epoxy-filled voids and the solid minerals. Specimen preparation techniques are similar to thin sectioning, where the sample is immersed in epoxy and later sectioned to a thickness of 0.5 to 1mm. The section is then polished by means of standard abrasive techniques. Both illumination and detection are confined to a single location on the specimen, and the resolution to 100nm is typically achieved. The use of single location illumination and detection also eliminates the problem of depth-of-field associated with optical microscopy. Penetration of the laser into geological samples is limited by the opacity of the minerals. This can be compensated for because geological samples can, if necessary, be illuminated at full laser intensity, unlike delicate biological samples which usually require a filter to reduce

laser intensity to a few percent of the original laser power. Using LSCM, Fredrich et al. (1995) successfully imaged the pore structure of rocks with various porosities. The method creates a three-dimensional image of the specimen, which is an advantage over surface techniques which only yield a two-dimensional image.

### 2.6.4 Methods of fabric characterization

Fabric can be classified according to the methods of measurement. Indirect methods of fabric measurement will classify fabric according to the physical property that is measured. These physical measurements can be related to a certain fabric, and this needs to be verified by visual means. There has been very little research on the relationship between physical properties and fabric, due mainly to the difficulty and the complexity of the factors involved in visual classification of fabric.

Qualitative characterization of soil fabric has been investigated extensively in the field of soil science, and thus geotechnical engineers tend to utilize the terms and definitions which have been applied by soil scientists (eg. Brewer and Sleeman, 1988). However, when describing fabric, geotechnical engineers generally prefer quantitative methods as these methods are unbiased and have some relevance to mechanical behaviour of soils.

Fabric of natural soils can be described as either single-grain or multi-grain fabrics. Single-grain fabrics are generally found in cohesionless soils while fine-grained soils are commonly found as multi-particle aggregates. Characterization of single grain fabrics can be done in terms of grain shape factor, grain orientation and inter-particle contact orientations (Ingles and Lafeber, 1966; Oda, 1972; Mahmood and Mitchell, 1974; Mitchell et al., 1976). The grain shape factor is the length to width ratio ($L/W$) of particles and can be presented in a histogram. Orientation of soil particles can be expressed in terms of the inclination of the particle axes to a set of reference axes (Mitchell, 1993). Thin sections are generally used to simplify the result to a single angle (the angle between the particle long axis to a reference axis). In

this case, the spatial orientations of the thin section are relative to the sample or deposit should also be considered as part of the description. Particle orientations are generally expressed by histogram or rose diagram. Examples of the rose diagrams are given in *Figure 2-12* (Cetin, 2004). The diagram illustrates change in pore orientation of a clay-mica sand mix during consolidation.

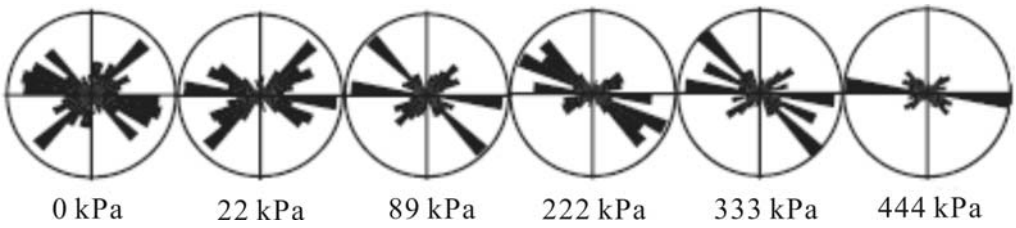


*Figure 2-12. Rose diagram of pore orientation during various stages of consolidation for a clay-mica sand mix (After Cetin, 2004)*

Single grain fabrics are rare in soils containing silt- and clay-sized particles because the particles are sufficiently small to be influenced by surface forces. In these cases, fabric is generally of a multi-grain nature. Mitchell (1993) also mentioned that silt-sized particles form multi-grain arrangements during slow sedimentation. This is reminiscent of the processes which take place in a tailings impoundment.

As pores are essential fabric elements, the characterization of pore size, shape and distribution is also an important part the soil fabric. Pore size, shape and distribution influence the conductive property, deformation behaviour and anisotropy of a soil (Mitchell, 1993). Pore shape and distribution can be characterized using image-processing techniques such as SEM. Volumetric pore size distribution can also be estimated using mercury intrusion.

The multi-grain nature of tailings makes characterizing fabric difficult. Characterization may require a combination of methods reviewed in this section. Statistical methods may also be an important tool.

To the best of the author's knowledge, the only research which included observation of soil behaviour as well as a direct measurement of fabric for the same material was presented by Wood (1999), who demonstrated that the difference in observed behaviour for samples prepared using different reconstitution methods was a result of grain contact as proposed by Yamamuro and Lade (1997). The theory proposes that three types of grain contacts exist in a sand-silt mixture. This is illustrated in *Figure 2-13*.

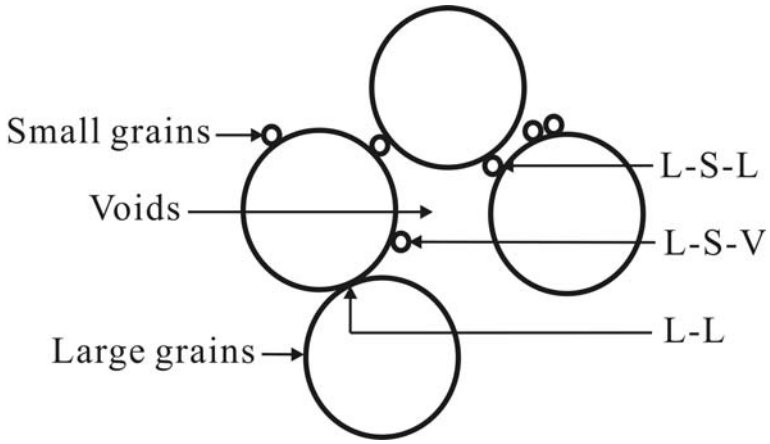


*Figure 2-13. Grain contact structure as proposed by Yamamuro and Lade (1997)*

Yamamuro and Lade (1997) postulated that stable contacts exist between large grains (L-L) while unstable contacts exist when large grains are bridged by small grains (L-S-L). Passive contacts occur when small grains rest on large grains without being part of the force chain. It is theorized that stable (strain hardening) behaviour is due in part to the presence of stable contacts (L-L) while significant presence of unstable contacts (L-S-L) results in unstable (strain-softening) behaviour.

Wood (1999) showed that for the same silt content of 10 percent, water sedimented samples, which showed strain hardening behaviour, contained significantly more stable contacts and less unstable contacts than the dry funnel deposited samples, which showed strain softening behaviour. A stability ratio, *S*, was also introduced which is expressed as the ratio of

percentage of stable to unstable contacts. If *S* is less than unity, an unstable response is expected either in the form of temporary or complete liquefaction, as illustrated in *Figure 2-14*.

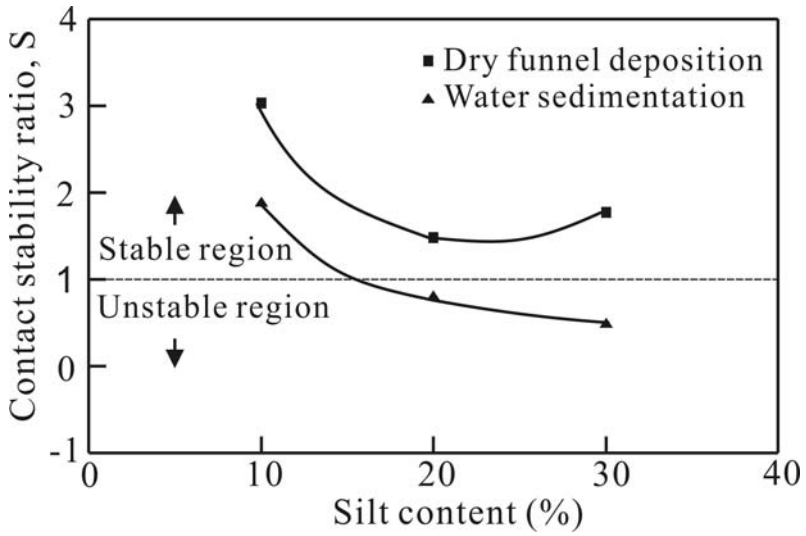


*Figure 2-14. Contact stability ratio, S, versus silt content for reconstituted sand-silt mix (After Wood, 1999).*

### 2.6.5 Concluding remarks regarding soil fabric

Although fabric and fabric effects is recognized as an important soil characteristic, methods of fabric classification is still insufficient, mainly due to the complexity of soils in general. As pointed out by Mitchell and Soga (2005), the variety of particle size, shape and distribution implies that the potential number of soil fabric is almost limitless. The method of fabric analysis will thus need to be adapted according to the observed fabric.

## 2.7 SAMPLE PREPARATION

The behaviour of a soil can be observed by soil testing, which can be divided into two main categories, namely in situ tests and laboratory tests. In situ tests have the advantages of testing in situ conditions such as structural features, pore water conditions and environmental effects, while laboratory testing can

be done under controlled conditions. Furthermore, laboratory specimens can be either undisturbed or reconstituted. Undisturbed specimens are brought into the laboratory in its in situ intact state, while reconstituted or remoulded specimens are prepared by remoulding natural material to break down particle associations, destroy shear planes or any structural features, eliminate large pores and create a more homogeneous specimen (Fearon and Coop, 2000). High quality undisturbed specimens are extremely difficult to obtain, as the natural structure of the soil can be altered during the processes of drilling, sampling, transportation, storage or specimen preparation for testing, due to changes in stress conditions, mechanical deformations, changes in water content or void ratio, or chemical changes (Clayton et al., 1995). In some cases, as is the case for tailings or some cohesionless sands, obtaining undisturbed specimens are difficult and sometimes impossible. Reconstituted specimens, on the other hand, can be easily obtained and re-constructed, but to obtain meaningful results, the specimen must replicate the in situ conditions as closely as possible. Burland (1990) suggested that a reconstituted sample should be made from a natural sample, mixed with water to form slurry, without drying the soil prior to mixing. The slurry should have moisture content between the liquid limit ($LL$) and $1.5LL$. It is then consolidated, preferably under one-dimensional consolidation. Ideally, the water used should have similar chemistry to the pore fluid.

Laboratory specimen reconstitution methods have some influence on the fabric and shear behaviour of the soil. Many researchers have shown that the behaviour of sands can be profoundly influenced by the sample reconstitution technique (Oda, 1972; Mulilis et al., 1977; Ladd, 1974, 1977; Vaid et al., 1999; Wood and Yamamuro, 1999). The energy used in reconstitution may also have an influence on the soil. Rippa and Picarelli (1977) showed that the Atterberg limits of a structurally complex soil were highly dependent on the preparation method. They believed that this was due to the breaking down of silt sized clay aggregates with increased remoulding energy. Fearon and Coop (2000) showed that the energy used in reconstitution of a specimen can alter the structure of scaly clay. They suggested that hand-mixing generally used for constructing laboratory test specimens produces a fabric similar to that of

natural clay while more vigorous methods of mixing may destroy the natural fabric of the clay.

### 2.7.1 Specimen reconstitution methods

Reconstituted specimens can be constructed using different preparation techniques depending on, among other factors, the soil type, moisture content, void ratio required and in situ fabric. Tamping and pluviation techniques are most commonly used in current practice (Vaid et al., 1999), while other techniques such as slurry deposition, mixed dry deposition, dry funnel deposition and wet sedimentation are used to better simulate field depositional conditions. For triaxial testing, specimens generally have a length to diameter ratio of 2, with diameters of 38, 50, 75 or 100 millimetres.

Reconstituted test specimens should be of high uniformity to reduce complexities in characterizing the soil. This is however not possible. As shown by Frost et al. (1998), even highly controlled air pluviated specimens show some degree of non-homogeneity of void ratio distribution. These authors suggest that global void ratio values may lead to errors in the results of liquefaction tests.

### 2.7.2 Tamping methods

Tamping techniques are also known as rodding techniques. The method involves compacting soil of known mass into a mould of known volume. The soil can be compacted dry, known as dry tamping, or the specimen can be constructed with certain moisture content, known as moist tamping. Compaction is generally done in layers for better uniformity. The method has a few advantages over other reconstitution methods. Firstly, the method is simple and can be completed in a relatively short time. Furthermore, there is greater control over the initial density of the specimen, because a required mass of soil is compacted into a volume, yielding the required void ratio or density. Finally, the range of void ratios that can be achieved is wider compared with other reconstitution methods due to capillary effects between

grains. There are contradicting views in the literature about the uniformity of tamped specimens. Researchers such as Mulilis et al., (1977), Vaid and Negussey (1988) and Vaid and Sivathayalan (2000) suggest that moist tamped sand specimens tend to be less uniform, while others like Sladen et al., (1985) and Chen and van Zyl (1988) found moist tamping to yield highly homogeneous samples.

### 2.7.3 Dry funnel deposition and water sedimentation

Dry funnel deposition involves deposition of dry material via a funnel into the bottom of a split mould. The material is then placed in the funnel, which is raised along its axis of symmetry. Sedimentation specimens are formed by placing the soil in a low energy state without any drop height. The method, shown in *Figure 2-15a*, is commonly used for testing silty sands (Ishihara, 1993; Lade and Yamamuro, 1997; Yamamuro and Lade, 1997; Zlatovic and Ishihara, 1997). In order to achieve higher densities, the split mould can be tapped periodically. This is known as tapped funnel deposition. Dense specimens can also be produced by raising the funnel rapidly (although still without any fall height) prior to tapping. This method of specimen preparation is known as the fast funnel deposition.

Water sedimentation, which is also known as water pluviation, is essentially similar to funnel deposition, but differs in that the soil, either dry soil (Tatsuoka et al., 1986; Ishihara, 1993; Zlatovic and Ishihara, 1998) or saturated soil (Wood, 1999), is deposited via a volumetric flask into water. The volumetric flask is filled with soil and water. As the soil flows out of the flask, equal volumes of water flow into the flask due to the suction within the flask as soil is displaced. The method is shown schematically in *Figure 2-15b*. The nature of the water into which the solid particles are deposited may also have an effect on the response of the soil. Vaughan (1997) reported on tests in which a fine silty sand was pluviated into water containing various amounts of colloid clay particles. He concluded that the colloid clay particles can significantly influence the relative density of the water pluviated specimens.

The deposition of tailings into a stationary pond may be similar to water sedimentation and thus results in a saturated, low density deposit.

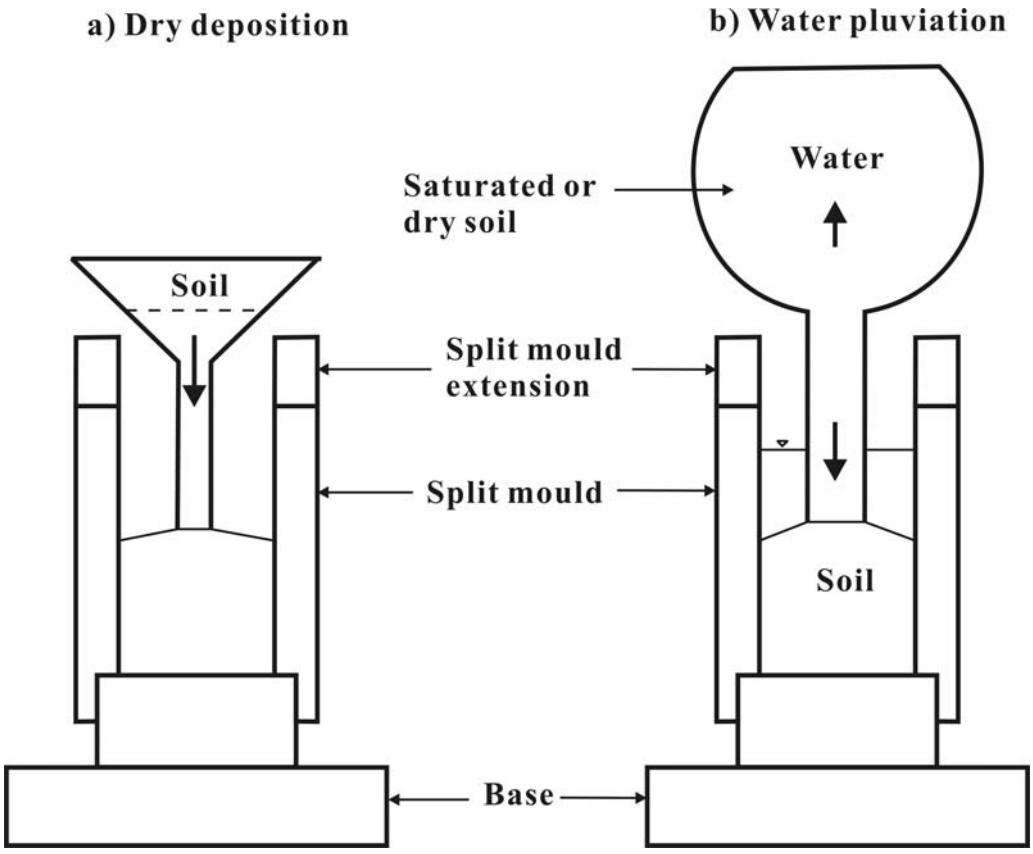


*Figure 2-15. Schematic representation of dry deposition and water pluviation (After Wood, 1999).*

Wood (1999) showed that dry funnel deposition and wet sedimentation produced silty sands specimens that exhibited a core and a shell structure. Silts reside more towards the periphery of the sample, and this is more apparent for the water-sedimented specimen. Furthermore, the silt content of the water-sedimented specimen increased from the bottom to the top of the specimen height. This is due to segregation of the different sized particles. Vaid et al. (1999) showed that in situ ground frozen specimens of sand behave very similarly to water pluviated specimens under triaxial and simple shear tests. They concluded that water pluviation can thus be used as an inexpensive and simple way of characterizing in situ fluvial and hydraulic fill sands. The in situ

void ratio of various sands were obtained from ground freezing techniques and compared with the loosest possible void ratio of water pluviated specimens (Vaid and Pillai, 1992; Vaid and Sivathayalan, 2000). They found that in situ sands deposited in water are unlikely to exist in states looser than the loosest achievable water pluviation specimens.

### 2.7.4 Slurry deposition and mixed dry deposition

The slurry deposition method was used by Kuerbis and Vaid (1988) and Kuerbis (1989), and was modified by Wood (1999). The method entails the use of slurry in a mixing tube, rotated for a certain amount of time. The mixing tube is then extracted slowly, leaving the slurry in the split mould. The mixed dry deposition is similar to slurry deposition, except that the soil is placed in a dry state. A schematic presentation is shown in *Figure 2-16.*

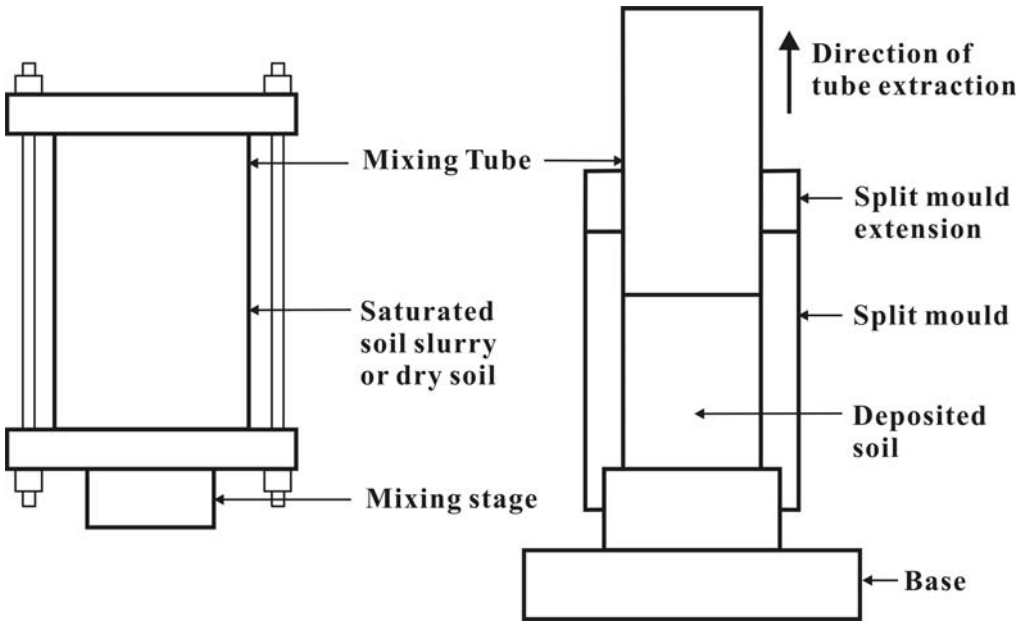


*Figure 2-16. Mixed dry deposition and slurry deposition (After Wood, 1999).*

Using silty sand, Wood (1999) showed that both slurry deposition and mixed dry deposition produce homogeneous specimens. Theron (2004) prepared a slurry sample using a mixture of fine platy particles and rotund sand. A three-

part split mould was installed on the triaxial pedestal and the sample was built on the pedestal. To prevent segregation, a layered approach was used. Slurry was deposited in thin layers and each layer was stirred before the new layer was deposited. This method allows slurry samples to be built for soils such as gold tailings, where segregation is possible.

### 2.7.5 Air pluviation method

Pluviation essentially involves raining dry soil from a fixed height through a long tube into the split mould. A variation in fall height and pouring rate is often used to create specimens of different densities (Miura and Toki, 1982; Vaid and Negussey, 1984, 1988; Rad and Tumay, 1987). A higher fall height creates denser specimens while a higher pouring rate decreases the density. In order to construct uniform specimens, Vaid and Negussey (1984) suggested that the fall height should remain constant with the top surface of the sample as it is formed.

Air-pluviated sand specimens were shown to contain alternating thin layers of loose and dense sand (Mulilis, 1977). Wood (1999) found that air-pluviated silty sand specimens show distinct thin horizontal silt layers, although the silt content was homogeneous throughout the specimen.

## 2.8 SAMPLING AND SAMPLING DISTURBANCE

In order to obtain reasonable engineering parameters for geotechnical design, carefully executed testing is required. Testing may either be in situ or laboratory tests, and in both cases, sample disturbance must be minimized. The mechanisms of disturbance can be classified as follows (Clayton et al., 1995):

- Changes in stress conditions
- Mechanical deformation

- Changes in water content and void ratio
- Chemical changes

These mechanisms can occur at various stages during the process of the investigation and at different rates. Although some disturbance is unavoidable, it can nevertheless be minimized by understanding the mechanisms involved and by careful design and execution of the testing procedures. There are three types of laboratory sampling techniques, namely (Clayton et al., 1995):

- Disturbed sampling: There is no attempt to retain the structural features of the soil and is adequate for classification tests.
- Tube sampling: The soil sample is obtained by pushing a tube into the soil. The soil is sheared, but integrity and structural features remain intact to some degree. Sampling disturbance from tube sampling can be minimized by careful design of the sampler. Samples obtained from tube sampling are considered 'undisturbed'.
- Block sampling: Samples are cut from the base or the side of a trail pit, or as part of a rotary drilling process. Block samples undergo stress relief and swell, but should not be subjected to shear distortion as with tube sampling.

In general, block sampling produces the highest quality undisturbed samples when compared with other sampling techniques (Heymann and Clayton, 1999).

## 2.9 SUMMARY

The state, composition and engineering behaviour of gold tailings have been presented. Tailings could be described as a low plasticity rock flour with coarse angular and fine platy particles (Vermeulen, 2001). The behaviour of gold tailings is recognized as somewhere between that of clay and sand, with fines dominating the mass (Pettibone and Kealy, 2971; Mittle and Morgenstern, 1975; Vick, 1990; Theron, 2004).

The method of reconstitution of tailings and soils in general has been shown to influence the mechanical behaviour. Investigations have generally concentrated on the liquefaction behaviour of granular materials. Questions such as consolidation, creep and small strain stiffness have seldom been mentioned. Furthermore, very little evidence has been presented to demonstrate that these observed differences in behaviour are in fact as a result of the different fabric.

With these questions in mind, an experimental methodology will be set up to evaluate the hypothesis: **Accurate simulation of the behaviour of gold tailings under laboratory conditions requires appropriate replication of the material fabric.**

# Chapter 3

# Experimental Methodology

## 3.1 BACKGROUND

The objective of this chapter is to present in detail the experimental work conducted during this project. This includes the reasoning behind the choice of tests and parameters used, descriptions of the experimental methods as well as of the equipment and instrumentation used in the testing.

## 3.2 EXPERIMENTAL STRATEGY

As mentioned in the opening chapter, material was sampled from a single tailings dam which had the same source. To ensure that the entire spectrum of gold tailings was investigated, material was sampled from three different positions on the tailings dam to represent typical gold tailings gradings. A few dams were considered, and finally it was decided that ERPM 4 would be the source of all gold tailings used in this research. The reasons for choosing ERPM 4 were that, firstly, the dam has been decommissioned for about 10 years, making sampling of pond material possible. Secondly, ERPM 4 had been constructed using the daywall-nightpan paddock system, typical of South African tailings dams.

The choice of a decommissioned dam, however, implied that oxidation may have occurred on the pyrite particles as a result of exposure to air (oxygen) and water (Blight and du Preez, 1997). Pyritic oxidation results in a reduction in pH (to acidic) near the surface of the dam and leaching of soluble salts of

approximately 0.1% by dry mass of tailings (Blight, 1976). Although fluid chemistry may have some influence on behaviour of gold tailings and on the fine platy particles in particular, it was assumed, as stated in section 1.3, that fluid chemistry only had an influence on the initial fabric, and not on the mechanical behaviour of the tailings.

The coarsest material (named upper beach) was sampled from the beach near the daywall while the finest material (named pond) was sampled near the penstock. Material with an intermediate grading (named middle beach) was also tested. The objective was to get some variation in the grading and particle shape characteristics of the material and to observe how this variation relates to fabric.

The main aim of the research was to compare mechanical behaviour of undisturbed and laboratory prepared (by moist tamping and slurry) gold tailings samples at the same state. Material from each position was tested at two effective confining stresses, 200 and 400kPa, to investigate the effect of confining stress. Desiccation suctions for general beach tailings were estimated to be in the range of 150kPa (Westraad, 2004**)**. It can thus be assumed that undisturbed samples will be normally consolidated above 200kPa as to eliminate the effect of over-consolidation. The testing included triaxial consolidation and shear, and as samples needed to be tested at the same state, consolidation and shear samples were tested separately. Details of the testing will be discussed in the following section. Coding for the test samples are summarized in *Table 3-1* and *Table 3-2*.

**Consolidation samples**

| | Undisturbed | Moist tamped | Slurry |
|---|---|---|---|
| Upper beach | UB-U-con | UB-MT-con | UB-S-con |
| Middle beach | MB-U-con | MB-MT-con | MB-S-con |
| Pond | P-U-con | P-MT-con | P-S-con |

*Table 3-1. Sample coding for consolidation samples.*

**Shear samples**

| | Undisturbed | Moist tamped | Slurry |
|---|---|---|---|
| Upper beach | | | |
| 200kPa | UB-U-200 | UB-MT-200 | UB-S-200 |
| 400kPa | UB-U-400 | UB-MT-400 | UB-S-400 |
| Middle beach | | | |
| 200kPa | MB-U-200 | MB-MT-200 | MB-S-200 |
| 400kPa | MB-U-400 | MB-MT-400 | MB-S-400 |
| Pond | | | |
| 200kPa | P-U-200 | P-MT-200 | P-S-200 |
| 400kPa | P-U-400 | P-MT-400 | P-S-400 |

*Table 3-2. Sample coding for shear samples.*

Abbreviations used in sample coding are summarized below:

- UB - Upper beach sample
- MB - Middle beach sample
- P - Pond sample
- U - Undisturbed sample
- MT - Laboratory prepared by moist tamping
- S - Laboratory prepared by the slurry method
- 200, 400 - Isotropic consolidation stress (in kPa) before shear
- con - Consolidation to 1000kPa effective stress

Test sample names are given as *material type-fabric type-confining stress*. P-U-200 would indicate an undisturbed pond sample sheared at an initial effective confining stress of 200kPa.

Undisturbed triaxial samples were cut from undisturbed blocks, which also provided information about the in situ void ratio and moisture content of the tailings. The moisture content used for preparing moist tamped samples was

determined from limiting density tests while that for slurry samples was established for all three material types by trial and error.

To compare the effect of fabric on the samples, it was important that samples were tested at the same initial state. Consolidation samples were at the same state prior to consolidation while shear samples were at the same state before and after consolidation and therefore throughout the shear processes, as the tests were undrained. The accuracy of the void ratio was within 2% of the target void ratio for all tests. The target void ratio was taken as the void ratio of the undisturbed sample, i.e. consolidation samples were at the same void ratios as the undisturbed sample after saturation. Shear samples were prepared to the same void ratios as the undisturbed sample after consolidation and creep.

For each test sample, a corresponding fabric sample was produced for fabric analysis. The fabric sample underwent the same triaxial processes as the test sample, without the final testing stage, to avoid modifications of the fabric. Consolidation fabric samples were removed after saturation while shear fabric samples were removed after creep at the corresponding effective stresses. This allowed the fabric to be compared immediately before the test phase (consolidation or shear). The void ratio of fabric samples was within 5% of its test sample counterparts. Fabric samples were given an extension '- f' added to the name of the corresponding test sample. MB-S-con-f therefore indicates a middle beach consolidation sample removed after saturation for fabric analysis. The triaxial testing scheme is summarized in *Table 3-3*.

Preliminary testing included indicator tests such as grading, specific gravity and Atterberg limits which gave some indication of the index properties of the gold tailings. Maximum and minimum density tests were also be performed on all three material types, at varying moisture content to aid in selecting appropriate moisture content for moist tamped samples. Sedimentation tests were performed with dispersant and flocculent to investigate the possible void ratios that could be obtained for slurry samples.

| | Test samples | | Fabric samples | |
|---|---|---|---|---|
| | Cons. | Shear | Cons. | Shear |
| Sample preparation | √ | √ | √ | √ |
| Flushing | √ | √ | √ | √ |
| Saturation against back pressure | √ | √ | √ | √ |
| Consolidation | √ | √ | | √ |
| Creep | | √ | | √ |
| Shear | | √ | | |

*Table 3-3. Triaxial testing scheme for the experimental work.*

Observation of the fabric was based on SEM images. SEMs were chosen over other indirect methods because, as a first step, the fabric difference must be observable to be comparable. A limitation with the use of SEM was that samples had to be dry before they could be examined in the SEM. This implied that samples had to undergo desiccation, which would induce some change in void ratio. As the samples were at the same void ratio, it is assumed that any changes in void ratio during desiccation would be similar, and would not significantly change the existing fabric.

## 3.3 SAMPLING

Pond samples were taken directly next to the penstock while the upper and middle beach samples were taken at approximately 20m and 45m away from the penstock respectively. The distance between the penstock and the daywall was approximately 50m. The three sampling positions are shown in the satellite image in *Figure 3-1*.

At each position, a hole of approximately one metre deep was dug in attempting to obtain a layer in excess of 100mm. The three sampled layers are shown in *Figure 3-2*. It should be noted from *Figure 3-2* that the gold yellow colour of the middle and upper beach material indicate pyritic oxidation.

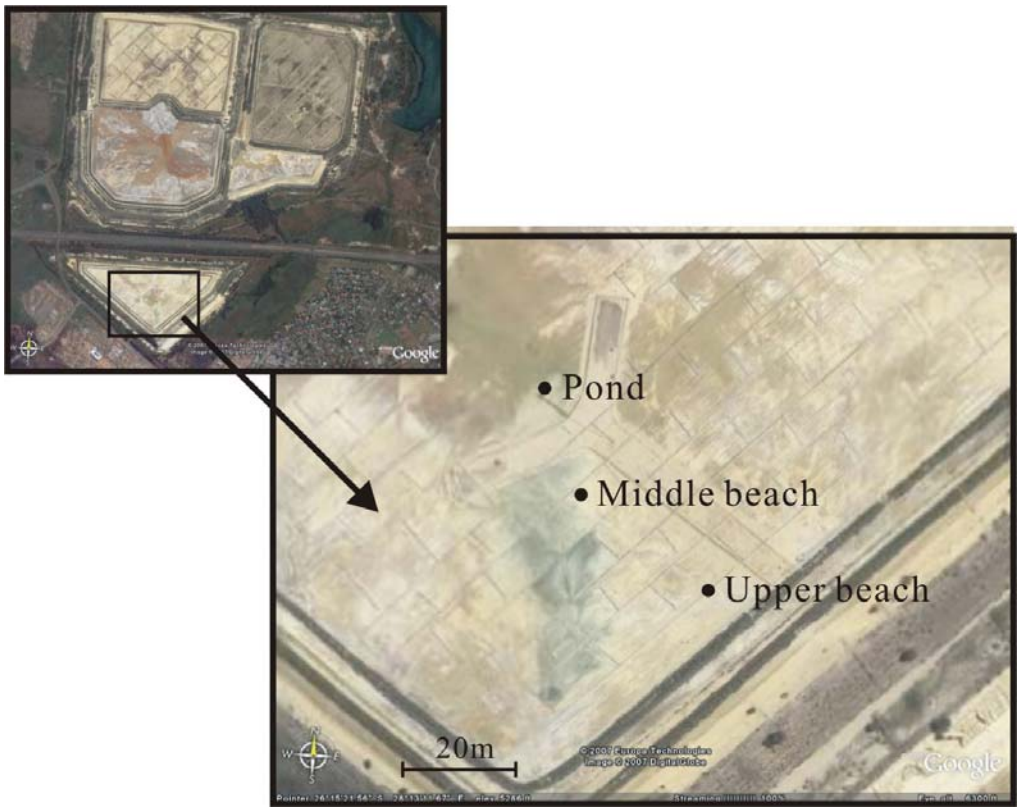


*Figure 3-1. Satellite view of sampling positions.*

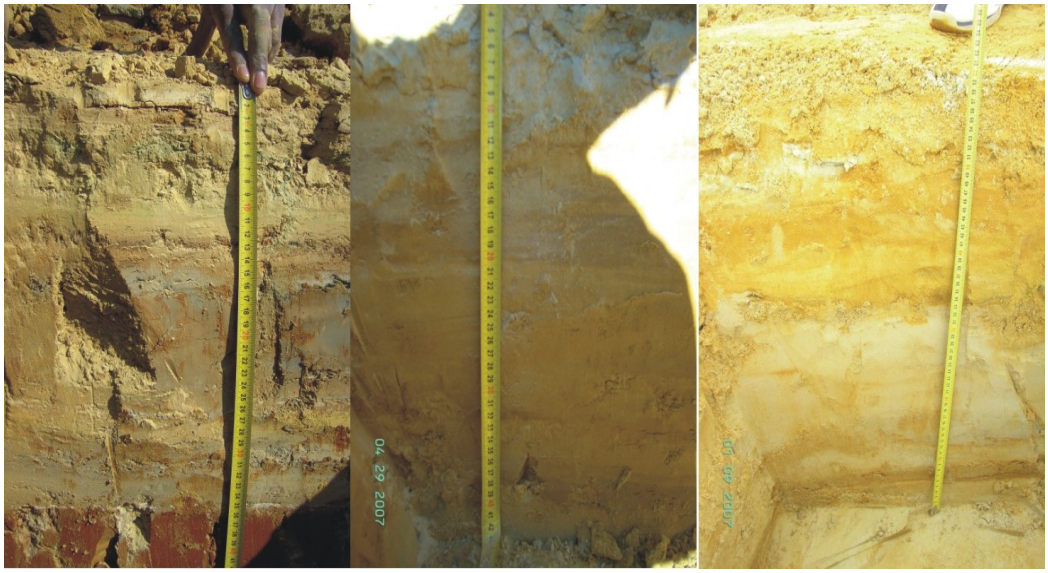

Pond Middle beach Upper beach

*Figure 3-2. In situ depth profile of block samples.*

Sample layer depth and layer thickness for the three materials are shown in *Table 3-4*. The table also includes visual descriptions of the three materials.

| | Layer depth | Layer thickness | Visual description |
|---|---|---|---|
| Pond | 150mm | 150mm | Grey fine clayey silt |
| Middle beach | 200mm | 200mm | Light brown sandy silt |
| Upper beach | 100mm | 170mm | Yellow sandy silt |

*Table 3-4. Position and visual description of undisturbed block samples.*

After a suitable layer had been targeted, the targeted block was exposed by removing the material above and around it, as shown in *Figure 3-3*. The block was then cut from the bottom and removed from its original position. The method is described by Clayton et al. (1995).


*Figure 3-3. Exposing a suitable block by excavating around the block.*

All samples were wrapped in plastic wrap and aluminium foil and finally another layer of plastic wrap to prevent moisture loss. This is demonstrated in *Figure 3-4*. The use of a plastic wrap/aluminium foil combination was shown

by Heymann and Clayton (1999) to be effective in minimizing moisture loss in undisturbed samples. The samples were then marked (top), hand-carried down the tailings dam and placed on foam mattresses for transportation back to the lab.


*Figure 3-4. Wrapping the block sample to prevent moisture loss.*

Average weather conditions for 30 days prior to sampling were obtained from 'Weather Underground' and are presented in *Table 3-5*.

| | Date sampled | Average temperature (ºC) | Total precipitation (mm) | Wind speed (km/h) | Humidity (%) |
|---|---|---|---|---|---|
| Upper beach | 9/1/07 | 20.8 | 148.6 | 4.2 | 61.7 |
| Middle beach | 30/4/07 | 17.0 | 45.0 | 3.3 | 58.6 |
| Pond | 1/9/06 | 11.4 | 28.4 | 0.3 | 53.3 |

*Table 3-5. Average weather conditions for 30 days before sampling*

Average weather conditions were included for reference purposes as the in situ moisture content may be affected by these factors.

## 3.4 PRELIMINARY TESTING

Preliminary tests were conducted to classify the material and to give some indication as to the behaviour that can be expected. The contents of preliminary testing mentioned in section 3.2 can be summarized as follows:

- Grading
- Specific gravity
- Atterberg limit
- Maximum and minimum density tests
- Sedimentation test using dispersant and flocculent
- Image analysis

Preliminary testing was done using the remaining disturbed material from the undisturbed blocks. All disturbed material (excluding that used for the Atterberg limit tests) was oven-dried at 50°C for 48 hours and passed through a 1mm sieve. The objective was to break down all existing fabric to present a truly 'disturbed' material. The methodology of the preliminary tests are discussed in the following sections.

### 3.4.1 Grading

Particle size distribution of the pond, MB and UB material was determined using procedures for wet sieving of fine non-cohesive material (BS1377: Part2:1990:9.3) followed by the hydrometer sedimentation test (BS 1377: Part 2:1990:9.5).

Wet sieving was done using 100g of dry material (as specified by BS for material smaller than 2mm) with sieves of 0.3, 0.15 and 0.075mm. Grading was done on both dispersed and undispersed material. The dispersed material was pre-treated with 100g of standard dispersant (35g sodium hexametaphosphate, 7g sodium carbonate and distilled water to make a one litre solution) because tailings are known to flocculate (Vermeulen, 2001,

Chang, 2004). Material passing the 75µm sieve was transferred directly to a measuring cylinder for hydrometer sedimentation test. Sieves were weighed before and weighed again with retained material after oven-drying. Sieving for each material was repeated twice.

Hydrometer analysis was done in four 1000ml cylinders (two for each material type and two for reference with distilled water and distilled water with dispersant). Cylinders were placed in a glass tank filled with water with a constant temperature of between 21 and 24°C. Corrections were made for the viscosity of water accordingly.

Test for calcareous matter was not performed, as carbonate bonding does not occur in tailings (Vermeulen, 2001). Organic pre-treatment on tailings was not used as hydrogen peroxide may also oxidize sulphide minerals such as pyrites (Vermeulen, 2001).

Vermeulen (2001) also suggested that sieve and hydrometer grading results were slightly finer when compared with the actual particle size as observed under the SEM. This is due to the fact that tailings contain flat and elongated particles which may pass through the square aperture of the tests sieves. Flat and elongated particles also do not adhere to Stoke's Law, which assumes spheres.

### 3.4.2 Specific gravity

The particle density or specific gravity of the tailings was determined for all three materials, although it is recognized that all tailings particles from the same source should have the same density (Vermeulen, 2001). Particle density was determined using the density bottle method specified by BS 1377: Part 2:1990:8.3. The density bottle test is suitable for soils consisting of particles finer than 2mm, as tailings particles generally are. The density bottles were washed, dried, cooled to room temperature and weighed to within 0.01g. Distilled, de-aired water was used for all density tests. As only one constant temperature bath was available, density bottles were placed in the same tank in

which the hydrometer analysis was done, and temperature correction for water density was made accordingly. The mass of density bottle only, density bottle and dry soil, density bottle and water, and density bottle with soil and water was determined and the particle density calculated.

### 3.4.3 Atterberg limit

Atterberg limits were determined for all three materials to allow classification of the tailings. For this, material was used at its natural moisture content (as specified by BS 1377:1990), as the plasticity properties of some soils may change due to drying. The liquid limit was determined using the cone penetrometer method (BS 1377: 1990:4.3). This method was chosen over the Casagrande method (BS 1377:1990:4.5) as it is less liable to experimental and operator errors (Sherwood and Ryley, 1968). The plastic limit was established using BS 1377: Part 2:1990:5.3. As tailings are not considered a cohesive material, determination of the plastic limit may not be possible, especially for the coarse material.

### 3.4.4 Maximum and minimum density test

Maximum and minimum density tests were performed to give an indication of the range of void ratios that can be expected for the tailings. Limiting densities can also be used as a guideline to minimize collapse and preserve the fabric for moist tamped samples during flushing. Maximum density was determined according to ASTM D4253-00 method 2A (maximum index density and unit weight of soils using a vibratory table), while minimum density was determined according to ASTM D4254-00. Both tests were modified to accommodate the testing of gold tailings. Both ASTM D4253-00 and D4254-00 require the material to be oven-dried and containing up to 15% particles by dry mass passing the 0.075mm sieve. Gold tailings contain mostly silt-size particles finer than 0.075mm, and the test was done at varying moisture content. The use of moist soil is contradictory to that specified in the standard test procedures and thus the results can only be used as a guide and not be compared with other standard limiting density results.

Material was compacted in a circular mould with an average internal diameter of 152.65mm and an average depth of 152mm. Surcharge load, including the base plate, was 25.63kg, which yielded a pressure of approximately 14kPa. The duration of the vibration was 8 minutes at 3600vpm at a peak-to-peak displacement of 0.33mm. Distilled water was used for all density tests. Moisture content ranges for different material types and the tests were terminated when the material liquefied and overflowed.

The minimum void ratio line (at various moisture content), together with visual uniformity assessment and practicality issues, were used as the basis on which the preparation moisture content for the moist tamped samples were determined. It is assumed that when the target void ratio lies on or below the minimum void ratio line, collapse during flushing can be minimized and the initial fabric can be preserved as best as possible. The choice of preparation moisture content is explained in detail in section 3.6.2.

### 3.4.5 Sedimentation test using dispersant and flocculent

Preparation of slurry samples may be a problem in that it is not always possible to prepare slurry or water sedimentation samples to the same void ratio as the undisturbed or moist tamped samples. There is less control over the void ratio for slurry samples compared with moist tamped samples and slurry or water sedimentation methods often yield denser samples. This was a difficulty for this project, as the void ratio at which the tests were started was important. Dispersant and flocculent were used to overcome this problem.

Sedimentation tests were done using dispersant and flocculent to observe the possible void ratios obtainable. Sedimentation tests were done for all three material types, with standard dispersant and flocculent concentrations of 0, 25, 50, 75 and 100% of the total fluid (mixed with tap water). Standard dispersant is defined as 35g sodium hexametaphosphate, 7g sodium carbonate and distilled water to make a one litre solution while standard flocculent is defined as 0.25g Magnafloc Mg 919 (supplied by Allied Colloids as a standard mining flocculent) diluted in one liter tap water. All samples were sedimented in

250ml cylinders with 100g dry material and 100g total fluid. Cylinders were shaken thoroughly and then shaken again for one minute immediately before the start of the test. Height readings were taken at 1, 2, 5, 10, 30, 60, 120, 240, 480, 1500 and 5000 minutes after commencement of sedimentation.

### 3.4.6 Image analysis

The objectives of the preliminary image analysis were, firstly, to observe if there were in fact any differences in the fabric of undisturbed and reconstituted tailings and, secondly, to evaluate the feasibility of different imaging techniques. Gold tailings used for the preliminary analysis originated in the Free State Goldfields, and was similar to that used by Chang (2004). Moist tamped and slurry samples were prepared at arbitrary void ratios for the preliminary test. Image analysis using raw intact samples and polished section samples showed that there was some observable difference in the fabric. Intact samples were viewed directly in the SEM and gave a three-dimensional image of the fabric while polished sections were prepared by immersing the intact samples with epoxy and polishing a section from the resultant epoxy block. The result was a binary image of either particle or epoxy (void). Two-dimensional (from polished sections) and three-dimensional (from raw intact samples) images are attached in *Appendix A* and summarized in *Table 3-6* below.

| Image | Description |
|---|---|
| A-1 | Moist tamped sample (raw intact) |
| A-2 | Moist tamped sample (polished section) |
| A-3 | Slurry sample (raw intact) |
| A-4 | Slurry sample (polished section) |
| A-5 | Undisturbed samples (raw intact) |
| A-6 | Moist tamped samples (raw intact moist taken in ESEM) |

*Table 3-6. Summary of preliminary electron microscopy images.*

From the preliminary images, it was decided that fabric analysis for this project would be based on SEM images of raw intact samples (similar to images *A-1* and *A-3* and *A-5*). The motivation was that, as a first step, the particle orientation should be observed physically and not be based on binary images or physical properties which cannot be directly observed. This would imply that classification of the fabric would be qualitative, as quantitative analysis of a three-dimensional was complex.

The reason for using image analysis was also to determine whether desiccation will alter the fabric of the samples. This was done by comparing images of raw intact samples using the conventional SEM and images from the ESEM (environmental SEM), which allows the use of moist samples. For this, moist tamped samples were prepared at various void ratios and imaged. The ESEM images show that moist tamped samples had similar fabric to that of naturally desiccated samples. This suggested that the initial fabric could be maintained after desiccation, and the use of SEM could be justified.

## 3.5 TRIAXIAL SETUP

The undrained shear behaviour of various samples was tested in a Wykeham Farrance 75mm triaxial cell. The base pedestal was modified to accommodate 50mm samples and local strain instrumentation. The cell was also modified to accommodate an internal submersible load cell. The experimental system is illustrated in *Figure 3-5*.

Pressure to the triaxial system was supplied by a compressor and converted to water pressure via an air-water interface. The cell pressure, however, was supplied by a digital pressure controller to allow a higher pressure to be applied to the cell fluid. Two lines led to the bottom of the sample while one line led to the top of the sample. Cell water was supplied through the cell valve. Pore pressure was measured at the bottom valve and volume changes measured through the top valve. The top valve was also modified to allow the

digital pressure controller to apply suction to slurry samples, and later during the test, to apply pressure to the cell fluid.

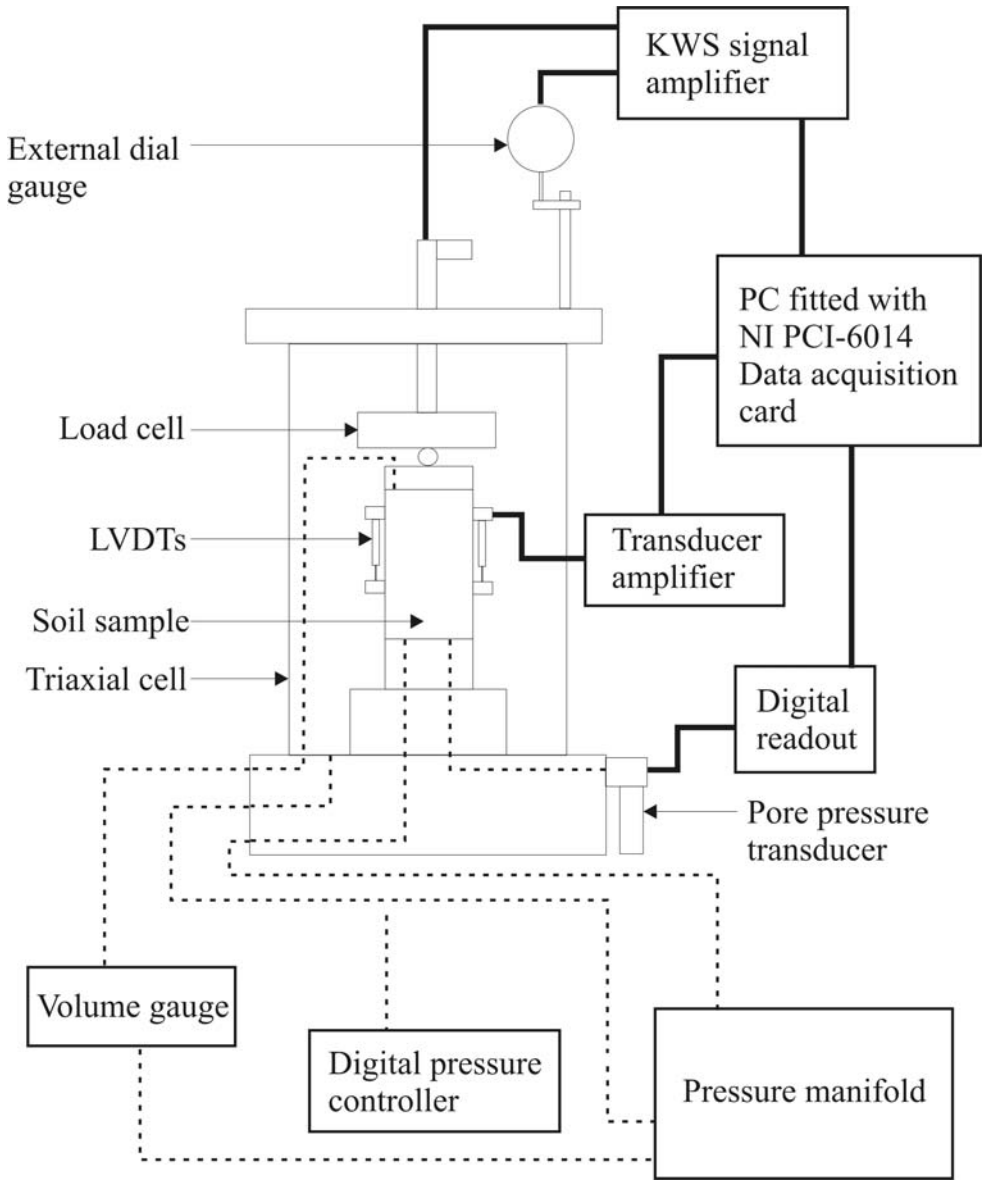


*Figure 3-5. The triaxial system and instrumentation.*

### 3.5.1 Instrumentation

Electronic instrumentation for the triaxial system included two LVDTs to measure local small strain deformation, a linear displacement transducer for large strain deformation, an Imperial College type internal submersible load

cell and an external pore pressure transducer. Output from these instrumentations were logged and stored on a computer via a NI PCI-6014 data acquisition card. The specifications of all electronic instrumentation as well as the data acquisition card are attached in *Appendix B*. Non-electronic instrumentations included a Budenberg Standard test pressure gauge and a Wykeham Farrance volume gauge. The instrumentation is discussed in detail in the following sections.

**Linear variable differential transformer (LVDT)**

The LVDTs used to measure local small strain deformation were obtained from RDP Electronics model D5/200 with a S7AC transducer amplifier. LVDTs were mounted onto the soil samples via brackets designed to fit 50mm samples. Calibration procedures for the LVDTs and other electronic instrumentation is discussed in the calibration section.

**Linear displacement transducer**

Large strain deformations were measured by a Kyowa linear displacement transducer (LDT) DT-20 D. Output signal was channeled through an HBM KWS 3073 signal amplifier, at a sensitivity of 1mV/V, and then logged by the computer.

**Internal load cell**

Deviatoric stress was measured via an Imperial College type internal submersible load cell (load capacity of 450kg) to eliminate ram friction from the measurements. The output signal was amplified via the same HBM KWS 3073 amplifier used for the external displacement transducer. The sensitivity setting for the internal load cell was set at 0.5mV/V.

**Pore pressure transducer**

Pore pressure was measured by a Genspec GS4200 pressure transducer which has a maximum output of 10V and a range of 1000kPa. Output was channeled through a custom made digital readout and finally recorded onto the computer.

**Pressure gauge**

With the exception of cell pressure (which was supplied by the digital pressure controller), all pressure used in the triaxial system were supplied by a traditional compressor which supplied constant air pressure of up to 550kPa. Air pressure was converted to water pressure via an air-water interface. Pressure was controlled using pressure regulators and read by a Budenberg standard test pressure gauge. The gauge had a capacity of 1700kPa and a resolution of 10kPa.

**Volume gauge**

Sample volume change measurements during saturation and consolidation were measured by a Wykeham Farrance burette type volume gauge, which has a 100 ml capacity and a resolution of 0.2ml.

### 3.5.2 Instrumentation calibration

All instrumentation was calibrated to evaluate the accuracy of the transducers. Transducers were calibrated against a suitable reference in order to establish the closeness of the outputs to the true values. According to authors such as Doebelin (1990), Collett and Hope (1983) and Sydenham (1982), the accuracy of the reference system should be 3 to 10 times that of the instrument being calibrated. A consistent calibration methodology (Heymann, 1998) was used to calibrate all instrumentation. The methodology included the following steps:

1. Calibration of the transducer (including signal conditioning unit and A/D converter) or apparatus against a suitably accurate reference.
2. A least squared linear transfer function was determined to describe the relationship between the measured quantity and the digital output.
3. Error was calculated for each calibration point as the difference between true value (engineering units) and the measured value converted to engineering units via the transfer function. Errors were plotted against true value to allow for visual assessment of measurement uncertainty.
4. The accuracy of each instrument was calculated as ±1.96 times the standard deviation of the errors. Assuming that errors are normally

distributed, this gave a confidence level of 95% that the difference between true values and measured values was within the specified accuracy.

Calibration data and graphs for all instrumentation are attached in *Appendix B*. The instrumentation was calibrated to ensure that the measurements were in an acceptable range. Factors such as accuracy, resolution, sensitivity, hysteresis and noise were quantified for each instrument. A brief description of these terms is given in *Table 3-7*.

| **Term** | **Description** |
|---|---|
| Accuracy | The closeness of measured value to the true value. |
| Resolution | Smallest division on the readout scale. In this thesis, resolution of logged data is restricted by the resolution of the data acquisition card (65536 bit per full range). |
| Sensitivity | Amount of output response per input quantity. |
| Hysteresis | The difference between the loading and unloading curves. |
| Noise | Random measurement variation caused by external factors. |

*Table 3-7. Terms used in defining measurement uncertainty.*

**LVDT calibration**

Before the calibration process, it is important to locate the electric zero of the instrument, as the sensitivity of the signal becomes non-linear further away from the electric zero. This was done by pressing the zero input button and adjusting the zero control to have a zero output. The LVDTs were calibrated over four gain (amplification) settings. Gain setting of 5 was used the measurement of all deformations prior to shearing. The gain was adjusted to 8 just prior to shearing commencing. During shear, the gain setting was gradually reduced from 8 through to 7, then 6 and finally back to 5 as axial strain increases.

Before calibration, the effects of armature position for the LVDTs were first evaluated. At a gain of 5 (coarse gain) it was found that for both LVDTs, a

linear relationship can be expected within a range of ±7mm of the electrical zero. At gains 6, 7 and 8, the output was linear throughout the entire physical range of the LVDT. The effects of armature position for both LVDTs are illustrated in *Figure B-1 to B-4* and *B-9 to B-12* in *Appendix B*. All measurements (irrespective of gain) were taken within the ±7mm range for this project to ensure that the linear transfer function was valid.

Two systems with contrasting benefits were used as a reference system. Firstly, YPG Tungsten Carbide gauge blocks with an accuracy of ±30nm at 20°C were used. The system, however, required the manual replacing of blocks during calibration. Potential errors from this calibration method occur as a result of the change in alignment of LVDT rods during placement and replacement of the gauge blocks. In addition, measurements could only be made at discrete intervals equal to the thickness of the gauge blocks. The second system was the use of a Mitutoyo micrometer. Calibration involves fixing the micrometer and the LVDT while adjusting the height of the lever arm via a height adjustment screw. This is demonstrated in *Figure 3-6*. The micrometer, however, had a lower accuracy of ±1.5µm in comparison with the gauge blocks. Measurements were also limited to the resolution of the micrometer of 1µm.

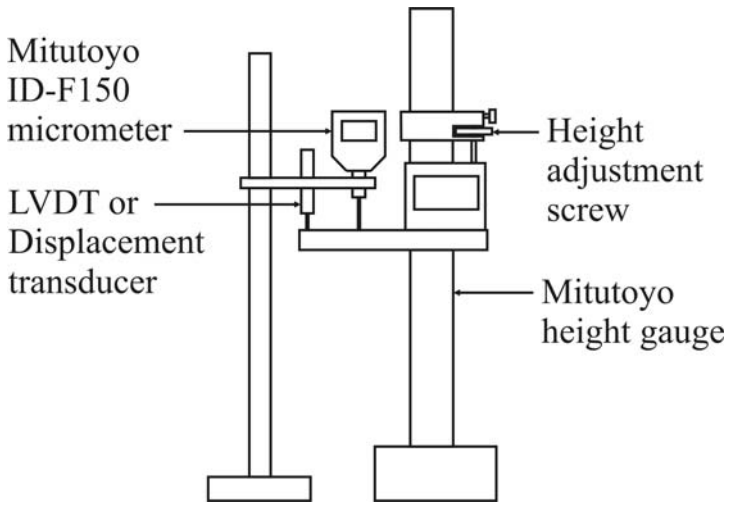


*Figure 3-6. Calibration setup for the LVDTs.*

It was originally decided that gain 8 would be used for small strain measurements. During trial tests, it was difficult keep the output within the range of the amplifier after the gain had been increased from 5 to 8. This requires that after deformation has taken place, the signal must be within the range of -0.9V to 0.45V on gain 5. This was sometimes not possible, as axial deformation would then require to be estimated with an accuracy of 1mm. This problem was solved by starting shearing at gains of either 6 or 7 when the armature position (after deformation) falls outside the range at gain 8. The use of gains 6 and 7, however, sacrificed output sensitivity and resolution for a larger workable range on gain 5. The workable ranges on coarse gain 5 for gains 6, 7 and 8 are summarized in *Table 3-8*.

| **Gain** | **6** | | **7** | | **8** | |
|---|---|---|---|---|---|---|
| | **Max** | **Min** | **Max** | **Min** | **Max** | **Min** |
| **LVDT 1** | 3.67V | -6.0V | 1.24V | -2.54V | 0.45V | -0.90V |
| **LVDT 2** | 3.74V | -6.0V | 1.25V | -2.53V | 0.46V | -0.88V |
| **Range** | ≈6.6mm | | ≈2.6mm | | ≈0.9mm | |

*Table 3-8. Working range for the two LVDTs at various gain levels.*

From *Table 3-8*, it can be seen that when the gain was decreased, the range within which axial deformations needed to be estimated increased. The accuracy, sensitivity and resolution of both LVDTs on all gain positions are summarized in *Table 3-9*. The linear transfer function was calculated from the micrometer calibration data as a higher accuracy was obtained when compared with the gauge block calibration data.

Calibration data for both LVDT1 and LVDT2 at gains 5, 6, 7 and 8 are illustrated in *Figure B-5* and *B-13* respectively. Errors for both LVDTs are plotted in *Figure B-6* and *B-14*. Loading and unloading plots of the two LVDTs on both coarse and fine gain are illustrated in *Figure B-7, B-8, B-15* and *B-16*. Hysteresis for LVDT1 on gains 5 and 8 were 0.06V and 0.4V. Calibration data for LVDT2 yielded a hysteresis on gains 5 and 8 of 0.04V and

0.4V respectively. The hysteresis on gain 8 is result of an offset of the height gauge during change in the direction of movement, and is evident from the constant values in the hysteresis graph for both LVDTs on gain 8. Hysteresis for the LVDTs on gain 8 is estimated to be 0.2V.

| Gain | Accuracy (µm) | | Sensitivity (µm/V) | | Resolution (µm) | |
|---|---|---|---|---|---|---|
| | LVDT 1 | LVDT 2 | LVDT 1 | LVDT 2 | LVDT 1 | LVDT 2 |
| **5** | 12.6 | 13.6 | 676 | 683 | 0.206 | 0.208 |
| **6** | 2.2 | 3.5 | 219 | 224 | 0.067 | 0.068 |
| **7** | 1.8 | 3.0 | 74 | 75 | 0.023 | 0.023 |
| **8** | 2.8 | 1.4 | 27 | 27 | 0.008 | 0.008 |

*Table 3-9. Accuracy, sensitivity and resolution for the two LVDTs at various gain levels.*

**LDT calibration**

Calibration of the linear displacement transducer used for external displacement measurements followed the same process as the LVDT calibrations, using both gauge blocks and the micrometer. In this case, it was evident that the gauge blocks showed a better accuracy than the micrometer, and thus the transfer function was determined from the gauge block data was used. The calibration range was limited to the capacity of the LDT, which was 20mm. The calibration graph shown in *Figure B-17* shows a sensitivity of 1.9786mm/V. The accuracy of the transfer function was calculated as 44µm. Error and hysteresis graphs are shown in *Figure B-18* and *B-19*. From *Figure B-19*, it was evident that some hysteresis was shown by the LDT. This was not considered a problem as no load/unload cycles was done during the experimental work. Resolution of the LDT is again restricted by the data acquisition card to approximately 0.6µm.

**Load cell calibration**

Before calibration took place, the load cell was checked for possible faults such as oil leakages and wiring. Calibration was done in a Lloyds LRX Plus

single column test system to a load of 1000N. For a 50mm sample, this amounts to a deviatoric stress of approximately 500kPa, which is sufficient for tailings samples, as demonstrated by Vermeulen (2001). Calibration data yielded a sensitivity of 102N/V and an accuracy of 7N. Calibration and error graphs are shown in *Figure B-20* and *B-21* respectively. No hysteresis was found, as loading and unloading plots were identical. The load cell could thus be interpreted with a resolution of 0.03N.

**Pressure instruments calibration**

Pressure instruments included the GDS digital pressure controller (which supplied the cell pressure), the pore pressure transducer and the Budenberg standard test pressure gauge on the pressure manifold. All pressure instruments were calibrated with the pressure transducer, which in turn was calibrated using the Budenberg 3/500 dead-weight calibration device. The reason for this indirect calibration was that the Budenberg test gauge was not movable and nor was the Budenberg dead-weight system.

Calibration involved first establishing a relationship between the pressure transducer and the Budenberg dead weight system (assumed to be the true pressure). The output (recorded by a computer), digital pressure controller and Budenberg standard test gauge were then calibrated against the calibrations of the Budenberg dead-weight system (via the pressure transducer). The relationship between the pressure transducer and the Budenberg 3/500 is shown in *Figure B-22*. Calibration ranges for output and digital pressure controller were restricted to the capacity of the pressure transducer (1000kPa). The Budenberg standard test gauge was calibrated to the capacity of the compressor (around 550kPa) *Figure B-23* illustrates the relationship between output, digital pressure controller and Budenberg standard test gauge outputs, and the true pressure as defined by the Budenberg dead-weight system. The errors for the three apparatus are plotted in *Figure B-24*. From the figure, it is evident that at low pressures, the Budenberg standard test gauge yields higher errors than at higher pressures. Accuracies and sensitivities are summarized in *Table 3-10.*

| Instrument | Accuracy | Sensitivity | Resolution |
|---|---|---|---|
| Output | 1.5 kPa | 100 kPa/V | 0.03 kPa |
| Digital pressure controller | 2 kPa | 1 kPa/kPa | 1 kPa |
| Standard test gauge | 4 kPa | 1 kPa/kPa | 10 kPa |

*Table 3-10. Accuracy, sensitivity and resolution for GDS, Budenberg and PC output.*

No hysteresis tests were conducted on any pressure apparatus.

**Volume gauge calibration**

Calibration of the volume gauge involved measurement of the weight of displaced de-aired water to a resolution of 0.1g (approximately 0.lml). The calibration method is similar to that used by Heymann (1998), and is demonstrated in *Figure 3-7*.

It is important that the volume gauge and all tubes are properly flushed and the de-aired water is of high quality. It is also important that the exit tube is submersed in water, as shown in *Figure 3-7*.

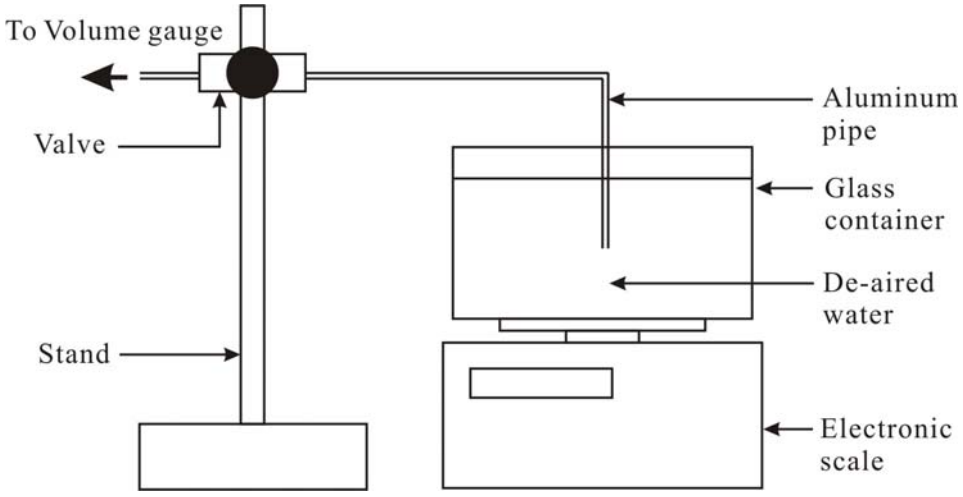


*Figure 3-7. Calibration setup for the volume gauge.*

The calibration range was restricted by the readability of the paraffin/water interface, and thus was calibrated in regions where the interface in the inner tube was clearly visible. The range was approximately 60ml. Calibration curve and error curve are shown in *Figure B-25 and B-26* respectively. Calibration data yielded accuracy for the volume gauge of approximately 0.2ml, with a resolution, also defined by the marking, of 0.2ml.

### 3.5.3 Measurement uncertainty

The calibration of the instrumentation aided in estimating the uncertainty of the computed parameters such as stress and strain. This section presents a brief discussion of the uncertainties in the analysis.

**Uncertainties in void ratio measurements**

The accuracy with which void ratios can be determined has been investigated by various authors (Vaid and Sivathayalan, 1996; Garga and Zhang, 1997 and Papageorgiou, 2004). They conclude that uncertainties in void ratio measurements can be caused by the following factors:

- Measurement technique
- Accuracy of the instrument and the precision of the operator
- Uncertainties in:
    - Sample height
    - Sample diameter
    - Sample weight
    - Specific gravity

Garga and Zhang (1997) investigated the uncertainty of void ratio measurements using aluminium dummies of known height and diameter, and concluded that the potential error in void ratio for a nominal 50mm x 100mm sample at a relative density of 30% using the calliper technique for height and diameter was 0.006 to 0.003. They further concluded that the uncertainty in

void ratio measurement as a result of the error in weight measurement is less than 0.01% and is thus negligible.

Papageorgiou (2004) investigated the uncertainties in void ratio measurements of gold tailings samples due to uncertainties in mass, height, diameter, volume and specific gravity at various initial void ratios and concluded that void ratio errors can be as high as ±0.08 for initial void ratios of up to 2. He further concluded that an increase in sample diameter and a decrease in initial void ratio can both reduce measurement uncertainties. It was also recommended that the void ratio of gold tailings samples measured using conventional measuring techniques (i.e. verniers, callipers, mass balances etc) can at best be quoted to 1 or 2 decimal places.

Taking into account the measuring instruments used, it was estimated that for the range of void ratios required for this thesis, the uncertainty of void ratio measurements were ±0.04.

**Uncertainties in stress measurements**

Stress is a measure of the intensity of force over a certain area, and thus both the uncertainties of area and force measurements must be taken into account. Force measurement errors are given by the load cell calibration data while area errors can be estimated from the accuracy of the measurement instrument, in this case, the Vernier calliper. Uncertainties in force measurements were estimated to be 6.4N while the error in area measurement is approximated to be 3.08mm², assuming a sample diameter of 50mm and a calliper accuracy of 0.01mm. This equates to uncertainties in stress measurements of approximately 6.5kPa in the calibrated load range.

During testing, changes in area could lead to changes in axial stress and thus area correction had to be considered in the stress calculations. The average cross-sectional area $A$ of the sample was obtained from *Equation 3-1*:

$$A = A_0 \frac{1-\varepsilon_v}{1-\varepsilon_a} \qquad \textit{Equation 3-1}$$

where $A_0$ is the initial area and $\varepsilon_v$ and $\varepsilon_a$ are volumetric and axial strains respectively. Under isotropic conditions, the axial strain in three directions is constant and $\varepsilon_v$ can be determined from *Equation 3-2*:

$$\varepsilon_v = (1-\varepsilon_a)^3 - 1 \qquad \textit{Equation 3-2}$$

Stress redistributions due to barrelling effects produced by rough platens during shear were not considered.

**Uncertainties in axial strain measurements**

For this research, three axial strain measurements were made during shear, namely using two LVDTs and an external linear displacement transducer (LDT). Axial strain is determined as the ratio of the change in length and the original length, and is given as a percentage. The accuracy of the LVDTs were estimated from calibration data as 0.012mm and 0.0021mm for gain settings of 5 and 8 respectively while the error of gauge length measurement for the LVDTs was the calliper accuracy of 0.01mm. The uncertainty in axial strain measurements from the LVDTs were then determined to be 0.047% and 0.008% for amplifier gains of 5 and 8 respectively. The accuracy of the LDT measurements was determined as 0.042mm in the range of 20mm. Uncertainties in axial strain measurements were therefore determined to be 0.082%.

## 3.6 LABORATORY SAMPLE PREPARATION

As mentioned in section 3.2, all disturbed samples (excluding those used for the Atterberg limit) were oven-dried at 50°C for 48 hours and passed through a 1mm sieve. Laboratory samples were prepared using two reconstitution techniques, namely moist tamping and slurry. The moist tamped method is the most commonly used laboratory preparation method that is suitable for all soil types. It is a simple method and target void ratios can be achieved with relative ease. However, there has been some evidence that the behaviour of moist tamped samples does not reflect in situ conditions. The other method, slurry

preparation, closely resembles the deposition of tailings, but difficulty of attaining the required target void ratio has generally been recognized. The two methods are discussed in detail in the following sections.

Before commencement of any testing, it was important that the triaxial cell was checked and de-aired. Preparation of the triaxial cell included flushing the top, back and pore pressure valves with de-aired water, de-airing the GDS pump and testing the membrane for leakage.

### 3.6.1 Undisturbed samples

Undisturbed samples were obtained from the undisturbed blocks. Plastic wrap and aluminium foil were carefully removed to expose the block. The block was first trimmed to fit into a soil lathe and then trimmed to a 50mm diameter sample in the lathe. After the sample had been trimmed to the required diameter, it was removed and trimmed to the required height of 100mm. Moisture content for the specimen was obtained from the trimmings. Procedures of sample preparation of the undisturbed samples are attached in *Appendix C*.

### 3.6.2 Moist tamped samples

The method of moist tamping has been described in section 2.7. The moisture content used for moist tamped samples was dependent upon:

- The position of the target void ratio in relation to the minimum void ratio at the specific moisture content. The moisture content was chosen so that the minimum void ratio was as close to the target void ratio as possible. It was assumed that collapse or swell would thus be minimized and the initial fabric preserved.
- The appearance of the sample. The moisture content was chosen to prevent the formation of lumps visible to the naked eye.

- Practicality. Sufficiently high moisture content was chosen so that samples had some strength during sample preparation and handling.

*Table 3-11* summarizes the preparation moisture content, minimum void ratio at the preparation moisture content, liquid limit and in situ void ratio.

| | Preparation moisture content (%) | Liquid limit (%) | In situ void ratio | Minimum void ratio |
|---|---|---|---|---|
| Pond | 25 | 51 | 1.42 | 1.68 |
| MB | 15 | 30 | 1.09 | 0.97 |
| UB | 7.5 | 25 | 0.61 | 0.62 |

*Table 3-11. Summary of preparation moisture content, minimum void ratio at the preparation moisture content, liquid limit, in situ void ratio for the three materials.*

Conventional moist tamping requires the material to be compacted using tamping rods. For this research, a hydraulic jack was used to compact all moist tamped samples in the mould. As the in situ void ratio lies on or close to the minimum void ratio, conventional compaction did not provide sufficient energy to compact samples to the target void ratio. Furthermore, at such a high density, moist tamped samples tend to crack when the mould is removed. Using a hydraulic jack allowed the compacted samples to be extruded from the mould.

Although all moist tamped samples were compacted using the hydraulic jack, the effort required to compact the samples to the target void ratio differed significantly with all three material types. Since measurements were available to quantify compaction effort, a comparative description is given. A significant effort was required to compact the moist tamped pond sample to the target void ratio. This may result in bending or breaking of the platy particles as well as disintegration of the flocks. Compaction of the moist tamped upper beach samples to the target void ratio required far less effort in

comparison with the pond samples. Moist tamped middle beach samples could easily be compacted using conventional moist tamping methods as described in section 2.7.2. An estimate of the force required at the handle of the hydraulic jack for compaction of moist tamped samples is given in *Table 3-12*.

| Material type | Pond | Middle beach | Upper beach |
|---|---|---|---|
| Force required (N) | 600 | 50 | 150 |

*Table 3-12. Estimate of force required for moist tamping.*

The procedures for preparing moist tamped samples are summarized below and illustrated in *Figure 3-8*. Photographs are included in *Appendix C*.

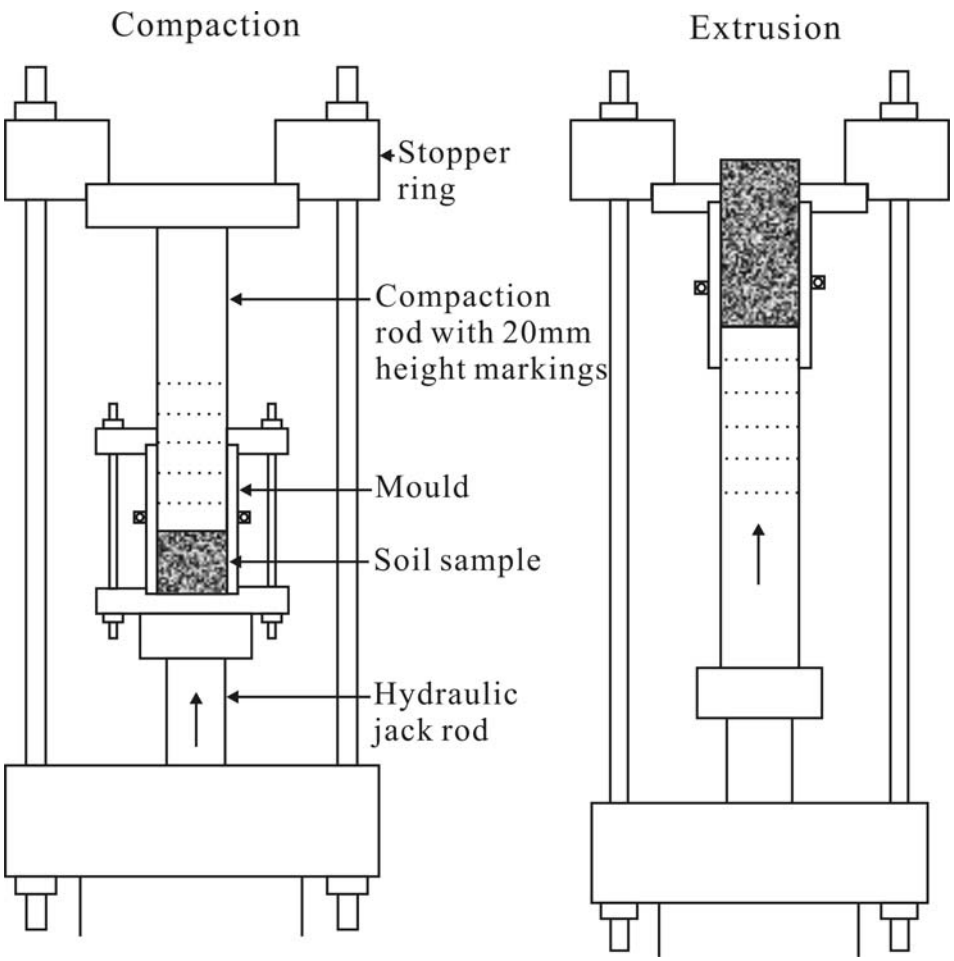


*Figure 3-8. Illustration of compaction and extrusion of moist tamped samples using a hydraulic jack.*

1. Dry tailings were weighed and mixed with the required moisture content (using tap water) and sealed in a closed container for 24 hours. This allowed the moisture to be distributed equally throughout the material. The material was mixed thoroughly again before use.
2. The total amount of moist soil for the target void ratio was determined. The amount of material to be deposited in each layer was then a fifth of the total amount.
3. The hydraulic jack and mould were setup.
4. The required amount of material was weighed and deposited into the mould. The material was compacted to the predetermined height marking (each layer is 20mm high). The surface of the previous layer was scratched before the next layer was placed. The procedure was repeated until the mould was full.
5. The sample was extruded from the mould.
6. Weight and dimensions of the sample were measured.
7. A moisture content sample was taken and weighed.
8. The bottom porous disk was placed on the base pedestal followed by the sample. The membrane was then stretched over the sample with a membrane stretcher. O-rings were then positioned over the base pedestal with an O-ring stretcher, holding the membrane tightly against the pedestal.
9. The top porous disk and the top cap were then placed over the sample, and the membrane was rolled over the top cap. Top O-rings were positioned over the top cap, holding the membrane over the top cap.
10. The brackets for LVDTs were then fixed onto the membrane using contact adhesive. The gauge length (distance between the top and bottom brackets) is approximately 50mm. Positions for the LVDT brackets were marked before the brackets were fixed. After the LVDTs had been positioned, the gauge length was measured again using a vernier calliper. The initial output for the LVDTs was also recorded.
11. The cell was then placed and fixed to the base, and the chamber filled with de-aired water.

### 3.6.3 Slurry preparation

For this research, slurry samples were prepared using a method similar to that described by Theron (2004). The decision on the appropriate preparation moisture content of slurry samples was not simple. Segregation can occur for slurries of high moisture content, resulting in alternating layers of coarse and fine material. On the other hand, slurries with low moisture content tend to trap air, resulting in cavities and a non-uniform sample. The initial idea was to prepare all slurry samples at moisture content just above the liquid limit to prevent segregation. This could be done with pond samples at a moisture content of 62% (1.2 times *LL*), but not with MB or UB samples. The void ratio for slurry samples prepared using MB and UB material were significantly lower than the in situ void ratio. For UB material, the highest void ratio achievable for a slurry samples was 0.5 while the in situ void ratio was around 0.6. MB slurry samples could be prepared at a void ratio of around 0.8 while the in situ void ratio was 1.1. Only a slight increase in void ratio could be achieved by increasing the moisture content of the slurry.

To solve this problem, dispersant and flocculent were added to the water used to prepare slurry samples. From the sedimentation tests, it was evident that the addition of dispersant or flocculent at specific concentrations can increase the void ratio. After some trial and error testing, it was decided that all UB slurry samples (including consolidation and shear) could be prepared to the required void ratio using 25% dispersant at a moisture content of 32% (just above the LL of 30%). MB slurry samples required a flocculent concentration of 50% for consolidation samples, 75% for shear samples consolidated to 200kPa, and 100% for shear samples consolidated to 400kPa. Moisture content was about 500%. This amounts to a moisture content/LL ratio of 17. Segregation was not a problem as the material settled in flocks and the excess water was removed using a syringe. An attempt was made to minimize the effects of the chemical additives by flushing out as much of these additives as possible. Once assembled in the triaxial cell, approximately three litres of water was flushed through each sample. This constitutes approximately 20 pore volumes of de-aired water. Flushing was done under a cell pressure of 25kPa and a back

pressure varying from 10kPa (at the deairator) and atmospheric (at the top drainage line).

The setup of the mould on the triaxial pedestal is demonstrated in *Figure 3-9*.

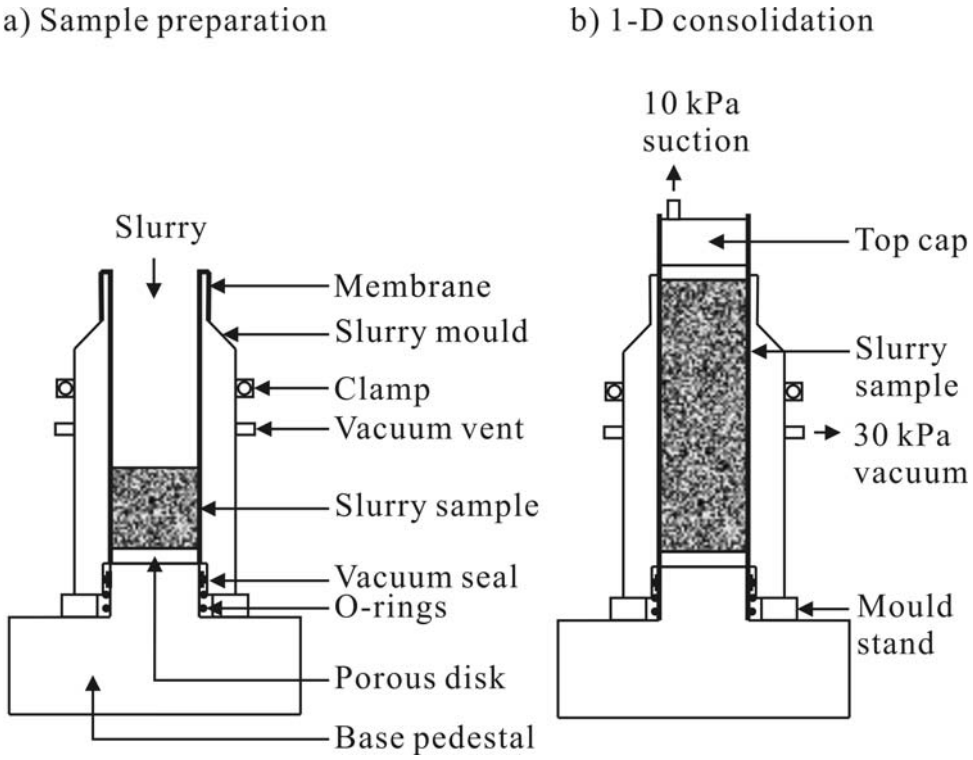


*Figure 3-9 Illustration of slurry preparation method.*

Procedures for the preparation of slurry samples are summarized below:

1. Tailings and tap water were first mixed in the required proportion to form enough slurry to fill the mould at the specific moisture content. The slurry mixture was de-aired in a desiccator for approximately 30 minutes.
2. The membrane was stretched over the triaxial base pedestal and O-rings were stretched over the membrane as shown in *Figure 3-9*. The bottom porous disk was then placed on the base pedestal. All porous disks were saturated before use.
3. The mould stand (two semi-circular parts) was placed on the pedestal followed by the sample mould (split mould). The mould was only placed when the vacuum seal for air suction was properly in place. The entire

mould was then clamped. The membrane was then stretched over the top of the mould and fastened in place via soft O-rings. This created an air-tight chamber between the membrane and the sample mould, and when the 30kPa vacuum was applied, the membrane was sucked tightly against the sample mould.

4. Slurry was then placed in the mould in thin layers. After each layer was placed, the top layer was stirred, without agitating the previous layer, to prevent segregation. Slurry was placed up to the top of the mould. The sample was approximately 100mm high.
5. After the slurry had been deposited, the top porous disk was placed, followed by the top cap. The membrane was then rolled over the top cap and O-rings were stretched over the top cap, holding the membrane tightly against the top cap.
6. 10kPa water suction was then applied through the top valve. This was done by adjusting -10kPa on the digital pressure controller. During the application of suction, the top cap was allowed to sink into the slurry mould, allowing some one-dimensional consolidation. This was required to maintain the cylindrical shape of the slurry sample. Once the pore pressure (measured at the bottom of the sample) had stabilized throughout the sample, the mould was removed.
7. Sample dimensions were then measured. Membrane thickness was deducted from diameter measurements. Sample weight was obtained by deducting the final mass from the original mass of the slurry.
8. A moisture content sample was taken and weighed.
9. Steps 10 and 11 for moist tamped samples were completed.

A detailed description with photographs for preparing slurry samples is attached in *Appendix C*

### 3.6.4 The effect of dispersant and flocculent

The use of laboratory preparation methods such as water pluviation or slurry deposition produces samples which duplicate the characteristic behaviour of natural soils and hydraulic fills (Oda et al., 1978; Vaid et al., 1999; Mao and

Fahey, 1999; Vaid and Sivathalayalan, 2000). It is well recognized by these researchers that these methods may produce samples of low void ratios.

Dispersant and flocculent were used in this research to achieve the target void ratios for slurry samples, after initial trials indicated that middle and upper beach slurry samples could not be prepared at the target void ratio using only tap water. The decision to use dispersant and flocculent was difficult as it was unclear what effects these chemical additives would have on the behaviour of gold tailings. It was decided that longer flushing times would be allowed to remove as much of the chemicals as possible and to minimize their effect on gold tailings behaviour. For these samples, approximately three litres of de-aired water, equivalent to approximately 20 pore volumes, was flushed through each sample.

Olson and Mesri (1970) conducted one-dimensional compression tests on various clays using different pore fluids. The concluded that the compression behaviour of clays such as muscovite, kaolinite and illite are dominated by mechanical bending, compressing and rupture of the particles coupled with shearing displacement at the contacts. Pore fluid chemistry influences the original soil structure of the clay, and thus has an indirect influence on th compression behaviour of the clay.

Mao and Fahey (1999) studied the effect of the flocculent Mg 919 on the behaviour of aragonite soil which is a silty calcareous soil obtained from below the seabed. According to Ruehrwein and Ward (1952), synthetic polymer flocculent such as Mg 919 are composed of long-chain molecules which adhere to the particles surfaces, binding them together physically to form stable flocs. The strength of these bonds is dependent on charge effects, dispersion forces or hydrogen bonding, and increases with molecular weight of the flocculent (Akers, 1975). Studies by Mao and Fahey (1999) indicate that the consolidation and shear behaviour are not affected by the addition of flocculent.

Anandarajah and Zhao (2000) investigated the stress-strain behaviour of kaolinite with various pore fluids. They concluded that pore fluids which decrease the repulsive barrier of particles may lead to an apparent over-consolidation in the specimen, and pore fluids which increase the net attraction of particles increase the cohesion of the specimen.

From the literature, it appears that the effect of dispersant and flocculent on the behaviour of gold tailings is minimal. Gold tailings consist of rotund and platy particles of quartz which is a stable mineral with no weakly bonded ions. Rotund particles are dominated by mechanical interaction due to the lower specific surface area. Platy particles in the clay size range may be affected by these surface forces, but it is assumed that the effect is only on the original fabric. Once the fabric is established, the behaviour of gold tailings is dominated by mechanical effects.

## 3.7 TRIAXIAL TESTING

The triaxial test was the standard consolidated undrained triaxial test. This included flushing, saturation under elevated back pressure, consolidation and shear. The triaxial testing procedure used in this research was performed according to the guidelines given in BS1377: Part 8:1990 and is summarized below.

1. After the sample was in place and the cell filled, the cell pressure was raised to 25kPa. The sample was then flushed by allowing de-aired water to flow (under a head of approximately 15kPa) from the back value, first through the bottom line (where pore pressure was measured) and then through the top valve. The objective of flushing was to remove as much air trapped in the sample as possible. The flushing process took approximately 24 hours. LVDT outputs were recorded to monitor volume change of the sample during flushing.
2. LVDT output was recorded at the end of each stage (flushing, saturation, consolidation and creep).

3. Saturation which followed the flushing process involved raising the pore pressure of the sample to dissolve trapped air into the water. To ensure saturation, samples must obtain a B-value of at least 0.95. B-value is determined as the ratio between the changes in pore pressure and changes in cell pressure. For this research, all samples were tested under a back pressure of either 300 or 400kPa.
4. Testing for this research required samples to be either consolidated or consolidated and sheared.
5. Consolidation samples were consolidated to an effective stress of 1000kPa. Consolidation samples were consolidated using a linear increase of cell pressure with time at a rate of 10 seconds per kPa.
6. Shear samples were first consolidated to an effective stresses of either 200 or 400kPa. 200kPa samples were consolidated following the standard consolidation procedure (by raising the cell pressure under undrained conditions and then opening the drainage to allow consolidation to take place) while 400kPa samples were consolidated using the same linear increase of 10 seconds per kPa as the consolidation samples.
7. Creep was allowed for 24 hours for all samples before shearing.
8. The creep rate was checked by closing the drainage for 10 minutes. It was expected that no excess pore pressure buildup should take place within the 10 minutes. If pressure build-up took place then the sample was left a further 24 hours to creep. No sample required a third 24 hour period to creep.
9. A constant rate of shear of 0.103mm/min was used for all tests. This was consistent with consolidation properties as determined from the shear-200 samples which were consolidated in the standard manner. The shear rate resulted to approximately 6% axial strain per hour.
10. Tests were terminated when a stresses have stabilized (at the critical state) or when further shearing could damage the LVDTs.

## 3.8 IMAGE ANALYSIS

Fabric of soils can be measured using various methods, each with its own benefits and limitations. As mentioned in section 2.6.3, methods of fabric measurement can generally be categorized into two main sections, namely visual methods and indirect methods. Visual methods are often based on image analysis of some image of the soil, while indirect methods, on the other hand, measure some physical property and relate the value to a certain fabric.

For this research, visual methods were chosen over indirect methods as a basis on which the fabric of tailings was compared. All samples were desiccated at room temperature. Fabric samples were constructed in the same manner as triaxial samples, but were removed before the test (consolidation or shear). Triaxial procedures for the fabric samples are summarized in *Table 3-3*.

It was further decided that raw intact samples would used for the SEM images. The reason for this was that three-dimensional images, although far more complex, give more detail and would aid in the understanding of gold tailings fabric.

### 3.8.1 Samples preparation for direct SEM

Fabric samples were viewed directly under the SEM. After desiccation, the samples taken from the triaxial were broken into smaller fragments to reveal the required surface. Care was taken to avoid the shear plane for the shear samples. Positions for SEM samples are shown in *Figure 3-10.*

Samples were mounted onto aluminium plates using conductive carbon paint. All samples were mounted with the orientation of the top noted. Care was taken to ensure that there was sufficient paint to hold the sample firmly. Extra carbon paint was used for MB and UB samples, as these samples were more brittle than the pond samples. The carbon paint was then allowed to oven-dry in a desiccator overnight. After the carbon paint had dried, the mounted sample was then further broken to reveal an undisturbed surface. Loose

material was gently blown away. The entire aluminium plate with the mounted samples was then coated with 5 layers (30nm) of gold (approximately 30 seconds per layer) using the sputter method. Coated samples could then be viewed in the SEM.

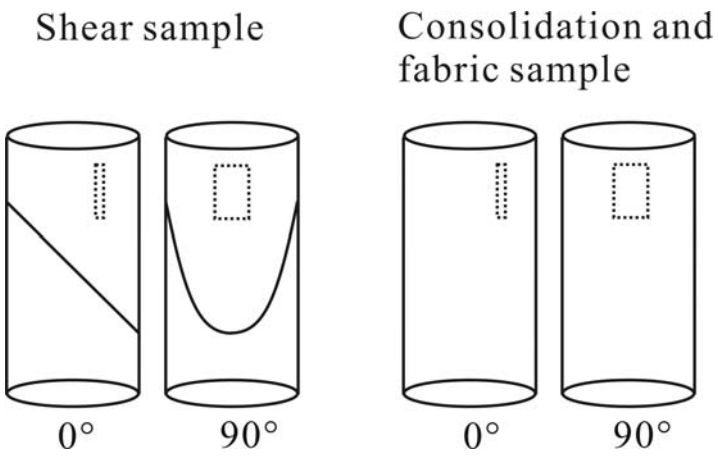


*Figure 3-10. Sample positions for SEM samples.*

### 3.8.2 SEM viewing

The SEM images were taken with a JOEL JSM-840 scanning microscope at a probe current of $3x10^{-11}$ amp, working distance of 12 mm and acceleration voltage of 5kV. Samples were placed in the vacuum chamber ($1 \times 10^{-5}$ torr) of the SEM. Two random positions were viewed at a magnification of 50, 200, 500, 1000 and 2000 times to examine the macro and micro fabric. Although random, positions were chosen where conduction was good to minimize charging effects. Charging effects (seen as bright lines or spots) could occur when electrons cannot drain through the carbon paint to the base. This was possible when the sample was too thick, or when the sample cracked or dislodged from the plate during desiccation or handling. Charging was generally a problem at higher magnifications as the entire electron beam is directed at a small area. Charged areas were avoided as far as possible.

## 3.9 CONCLUSION

An experimental programme was designed to investigate the effect of fabric on the consolidation, creep, shear and small strain behaviour of gold tailings. This included testing undisturbed and laboratory reconstituted gold tailings specimens obtained from various positions on ERPM 4 dam. The fabric was viewed under the SEM and these images form the basis of the fabric analysis.